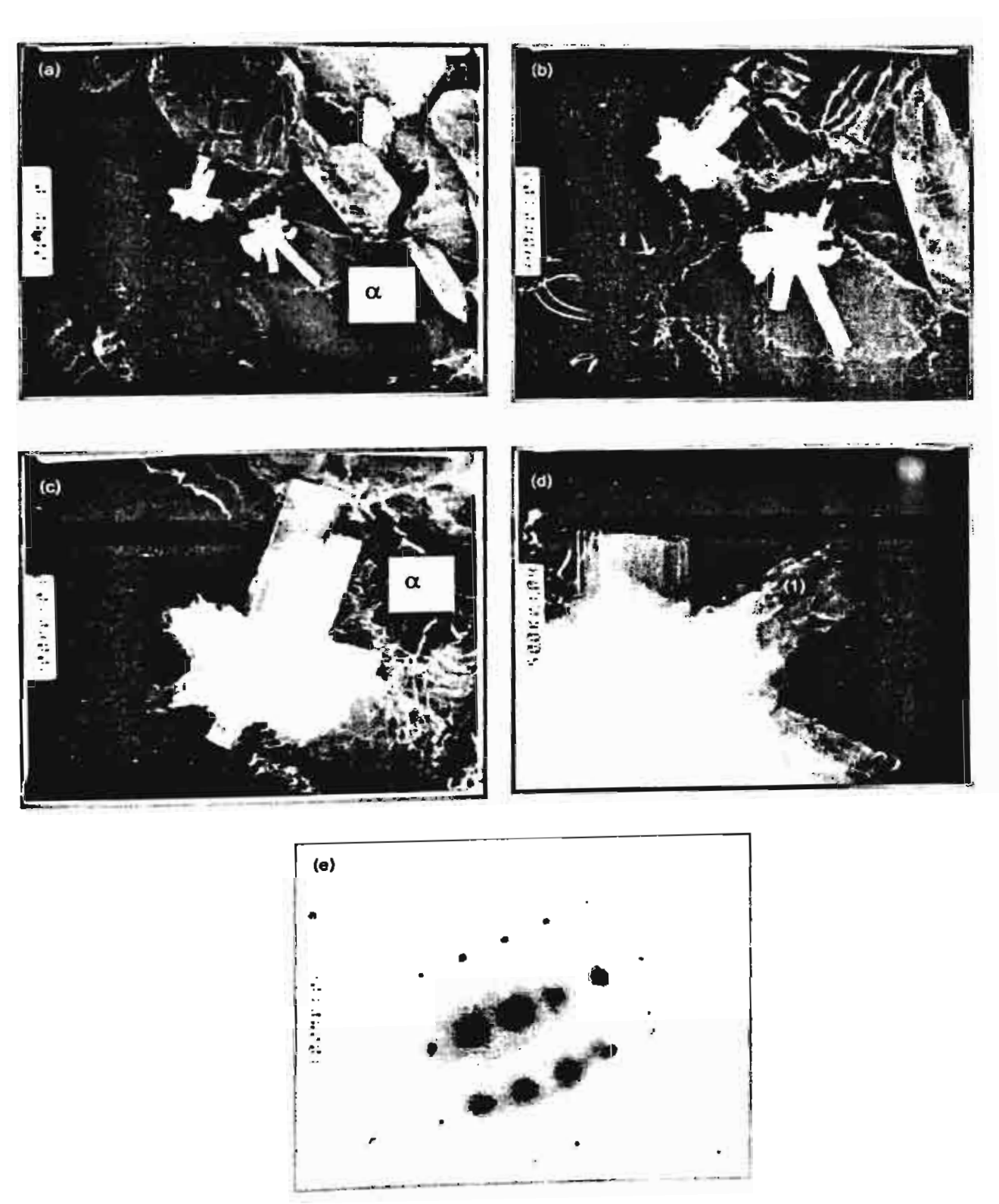
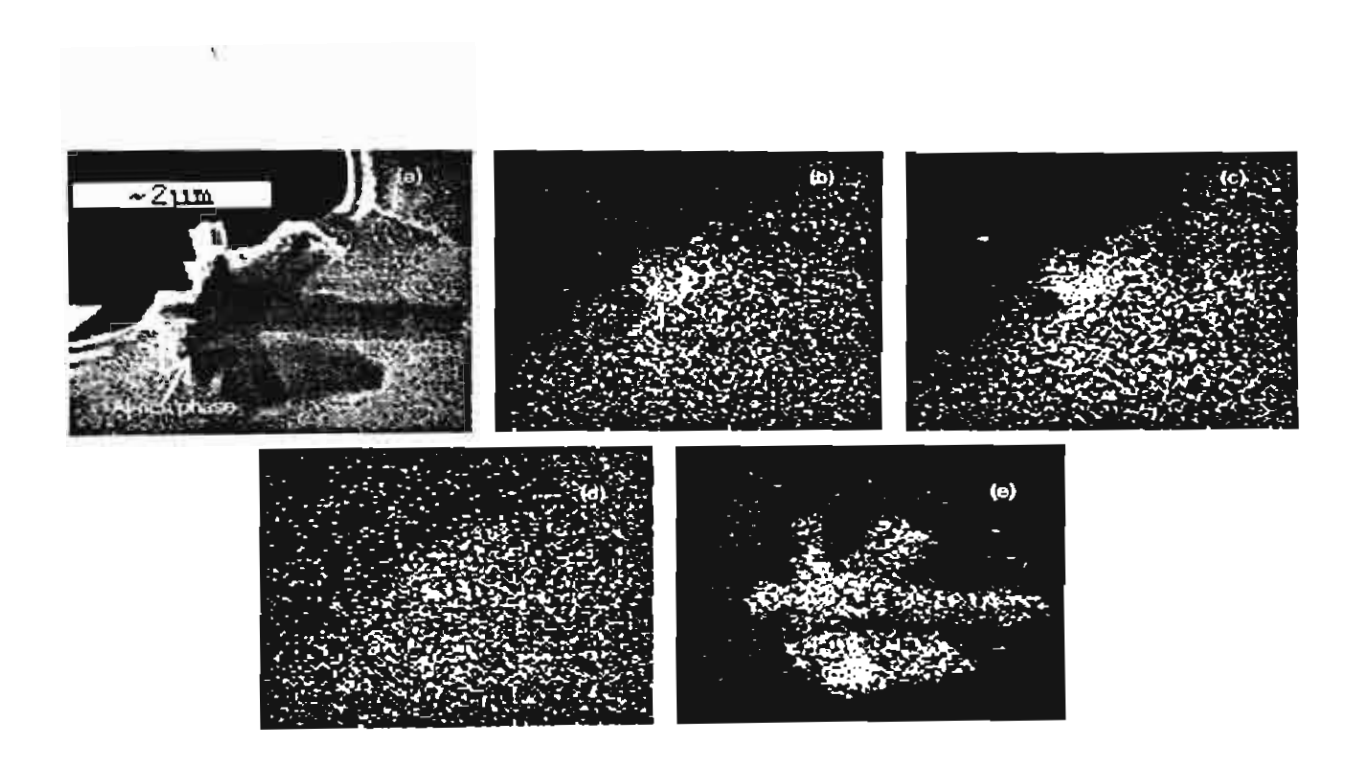


รูป 29 ภาพ ungat tietts (a) และ (b) แลดงยูเท็กติกคาร์ไบด์และอนุภาคคาร์ไบด์ขนาดเล็กซึ่งมีภาคตัดขวาง เป็นเอกซะแกนยด ในเหล็กหล่อ II (c) คือแบบรูปการเลี้ยวเบนจากเมทริกซ์ อื่นยันว่าเป็นเฟอร์ไรต์ (α)

อนุภาคที่มีขะลูมิเนียมสูงแสดงดังรูป 30 ซึ่งจะเห็นว่ามีลักษณะเป็นกลุ่มของผล็กซึ่งเกิดนิวเคลียสใน ตำแหน่งเดียวกันและโดออกไปในแนวรัคมี แบบรูปการเลี้ยวเบนในรูป 30(e) กำลังอยู่ในระหว่างการวิเคราะห์ ผลจาก scanning transmission electron microscopy (STEM) พบว่า การกระจายตัวของธาตุต่าง ๆ ได้แก่ Cr. Fe. V และ Al ในกลุ่มผลึกดังกล่าวไม่เป็นเนื้อเดียว ดังรูป 31 ซึ่งขึ้นยันความเป็นไปได้ว่ากลุ่มอนุภาคดัง กล่าวประกอบด้วยผลึกหลายชนิดขยู่ร่วมกัน



รูป 30 (a) -(d) คือภาพ bright field ของเหล็กหล่อ II แสดงอนุภาคที่มีอะลูมิเนียมสูงภายในเมทริกซ์เพ่อร์ไรต์ (e) แบบรูปการเลี้ยวเบนที่ได้จากบริเวณ (1) ของรูป 30(d)



ภูป 31 (a) ภาพ STEM ของอนุภาคที่มีอะลูมิเนียมสูงในเหล็กหล่อ II และ X-Ray dot maps (b) Cr Kα (c) Fe Kα (d) V Kα และ (e) Al Kα

### 4.2 เหล็กหล่อ 30wt%Cr-2.4wt%C-0.5wt%Mo-(1-3wt%)V

- โครงสร้างจุลภาคของเหล็กหล่อ 30wt%Cr-2.4wt%C-0.5wt%Mo-(1-3wt%)V ประกอบด้วยเดนไดรต์
  ของเฟอร์ไรต์ปฐมภูมิ และโครงสร้างยูเท็กติกขึ่งประกอบด้วยยูเท็กติกเฟอร์ไรต์และยูเท็กติกคาร์ไบด์
  M<sub>7</sub>C<sub>3</sub> การปรับสภาพด้วยความร้อนมีผลต่อโครงสร้างจุลภาคน้อย
- 2. การศึกษาด้วย Electron Probe Microanalysis ยืนยันได้ว่า Mo ละลายอยู่ทั้งในเมทริกซ์เฟอร์ไรต์และ ยูเท็กติกคาร์ไบด์ ส่วน V ส่วนใหญ่ละลายอยู่ในยูเท็กติกคาร์ไบด์
- สัดส่วนโดยปริมาตรของยูเท็กติกคาร์ไบด์อยู่ในช่วง 20-25 vol% และในกรณีที่ไม่มี Mo มีแนวโน้มเพิ่ม
   ขึ้นตามการเพิ่มขึ้นของปริมาณ V ส่วนในกรณีที่มี Mo ความแตกต่างมีนัยสำคัญน้อย
- 4. การศึกษาด้วยจุลทรรศนศาสตร์อิเล็กตรอนแบบสองผ่าน พบอนุภาคคาร์ไบด์ M<sub>7</sub>C<sub>3</sub> ขนาดเล็ก กระจาย อยู่ทั่วไปในเมทริกซ์เพ่อร์ไรต์ และพบอนุภาคที่มีอะลูมิเนียมและวาเนเดียมสูง รูปร่างคล้ายดาว เชื่อว่า น่าจะเป็นกลุ่มของอนุภาคที่ตกตะกอนอยู่ร่วมกัน ซึ่งกำลังอยู่ในระหว่างการศึกษาด้วย Electron Energy Loss Spectrometry ร่วมกับแบบรูปการเลี้ยวเบนของอิเล็กตรอน

### เอกสารอ้างอิง

Demello, J. D. B., Charre, M. D. and Thibault, S. H., Metallurgical Transactions, 14A, 1983, 1793.

Dupin, P., Saverna, J. and Schissler, J. M., AFM Transactions, 90, 1982, 711.

Fiset, M., Peev, K. and Radulovic, M., Journal of Materials Science Letters, 12, 1993, 615.

Gundlach, R. B. and Parks, J. L., Wear, 46, 1978, 97.

Hann, S. K. and Gates, J. D., Journal of Materials Science, 32, 1997, 1249.

Kibble, K. A. and Pearce, J. T. H., Cast Metals, 8, 1995, 123.

Kibble, K. A., M.Phil. Thesis, University of Wloverhampton, UK, 1987.

Pearce, J. T. H. and Elwell, D. W. L., Journal of Materials Science Letters, 5, 1986, 1063.

Pearce, J. T. H., AFS Transaction, 92, 1984, 599.

Pearce, J. T. H., British Foundryman 78, 1985, 13.

Pearce, J. T. H., Ph.D. Thesis, University of Aston in Birmingham, UK, 1982.

Pearce, J. T. H., *Proceeding of The Sixth Asian Foundry Congress*, Culcatta, India, Jan 23-26, 1999, 120.

Pearce, J. T. H., The Foundryman 95, 2002, 156.

Peev, K., Radulovic, M. and Fiset, M., Journal of Materials Science Letters, 13, 1994, 112.

Powell, G. L. F., Journal of Materials Science, 27, 1992, 29.

Radulovic, M., Fiset, M. and Peev, K., Journal of Materials Science, 29, 1994, 5085.

Rivlin, V. G., International Metals Revies, 29, 1984, 299.

Tabrett, C. P., International Materials Reviews, 41, 1996, 59.

### 5. ผลงานจากงานวิจัย (Output)

### 5.1 ผลงานวิจัยที่ตีพิมพ์ในวารสารวิชาการระดับนานาชาติ

- A Microstructural Study of Destabilised 30wt%Cr-2.3wt%C High Chromium Cast Iron ส่งดีพิมพ์ใน The International Journal of the Iron and Steel Institute of Japan (ISIJ International) (ดูภาคผนาก 2)
- 2. Electron Diffraction and Electron Energy Loss Study of High Chromium Cast Iron คาคว่าสามารถส่งตีพิมพ์ได้ภายใน 3-6 เดือน

### 5.2 ผลงานนำเสนอในงานประชุมวิชาการระดับนานาชาติ

1. Effects of Heat Treatment on Microstructure and Hardness of 30%Cr-2.4%C Cast Iron เสนอในงานประชุมวิชาการจุลทรรศนศาสตร์อาเซียน ครั้งที่ 3 ณ โรงแรมปางสวนแก้ว จังหวัดเชียงใหม่ ระหว่างวันที่ 30 มกราคม 2545 ถึงวันที่ 1 กุมภาพันธ์ 2545 ภาคโปสเตอร์ และได้รับรางวัลต่าง ๆ ดังนี้ (ตูภาคผนวก 1)

- รางวัลที่ 3 โปลเตอร์แสดงผลงานสาขาวัสดุศาสตร์

รางวัลชนะเลิศ ภาพถ่ายจุลทรรศนศาสตร์อิเล็กตรอนแบบส่องกราด

- รางวัลชมเชย ภาพถ่ายจุลทรรคนศาสตร์แสง

Characterisation of High Chromium Cast Irons
 เสนอในงานประชุมวิชาการ The 8th Asian Foundry Congress ระหว่างวันที่ 13-14 ตุลาคม 2546
 ณ โรงแรมมีราเคิลแกรนด์ กรุงเทพมหานคร ภาคบรรยาย (คุภาคผนวก 3)

### 5.3 การนำผลงานไปใช้ประโยชน์เชิงสาธารณะและเชิงวิชาการ

ได้มีความร่วมมือกับหน่วยปฏิบัติการการหล่อโลหะ ศูนย์เทคโนโลยีโลหะและวัสดุแห่งชาติ ภาควิชา
วิศวกรรมอุตสาหการ คณะวิศวกรรมศาสตร์ มหาวิทยาลัยเทคโนโลยีพระจอมเกล้าธนบุรี ในการ
เตรียมโลหะหล่อ และกลุ่มผู้วิจัยประสงค์จะสานต่อความร่วมมือในการศึกษาโครงสร้างจุลภาคของ
โลหะหล่อกลุ่มอื่น ๆ โดยมีแนวคิดจะทำในลักษณะของฐานข้อมูลตอไป

### 4. สรุปผลการทดลอง

### 4.1 เหล็กหล่อ 30wt%Cr-2.4wt%C

- โครงสร้างจุลภาคของเหล็กหล่อ 30wt%Cr-2.4wt%C จากการหล่อ (as cast) ประกอบด้วยเดนไดรต์ ของออสเตนในต์ปฐมภูมิ และโครงสร้างยูเท็กติกซึ่งประกอบด้วยยูเท็กติกออสเตนในต์ (ที่บางส่วน กลายเป็นมาร์เทนไซต์) อยู่ร่วมกับยูเท็กติกคาร์ไบด์ M,C,
- 2. โครงสร้างจุลภาคของเหล็กหล่อ 30wt%Cr-2.4wt%C ภายหลังการปรับสภาพด้วยความร้อนในช่วง 900-1100 °C เป็นเวลา 2-8 ชั่วโมง และทำเย็นในอากาศ ประกอบด้วยคาร์ไบด์ทุติยภูมิ M<sub>23</sub>C<sub>6</sub> ตก ตะกอนอยู่ในเมทริกซ์มาร์เทนไซต์ และอาจมีออสเตนในต์คงค้างบางส่วน ส่วนยูเท็กติกคาร์ไบด์ M<sub>7</sub>C<sub>3</sub> บางส่วนกลายสภาพเป็น M<sub>23</sub>C<sub>6</sub> เกิดเป็นโครงสร้าง core-shell
- สัดส่วนโดยปริมาตรของคาร์ไบด์ทุติยภูมิที่เกิดจากการปรับสภาพด้วยความร้อน อยู่ในช่วง 10-20
   vol% ช่วงอุณหภูมิและเวลาปรับสภาพด้วยความร้อนที่ใช้ในงานวิจัยนี้มีนัยสำคัญน้อยต่อสัดส่วนโดย ปริมาตรของคาร์ไบด์ทุติยภูมิที่เกิดขึ้น
- 4. การปรับสภาพด้วยความร้อนที่อุณหภูมิสูง ลดจำนวนต่อหน่วยพื้นที่ของคาร์ไบด์ทุติยภูมิ และเวลาการ ปรับสภาพด้วยความร้อนที่นานกว่าในช่วงอุณหภูมิไม่เกิด 950 °C มีแนวโน้มจะเพิ่มจำนวนคาร์ไบด์ ทุติยภูมิ
- 5. ลัดส่วนของ M<sub>23</sub>C<sub>6</sub> ภายในยูเท็กติกคาร์ไบด์หลังการปรับสภาพด้วยความร้อน อยู่ในช่วง 20-99 vol% เพิ่มขึ้นตามการเพิ่มขึ้นของอุณหภูมิการปรับสภาพด้วยความร้อน และที่เวลานานพอ สัดส่วนโดย ปริมาตรของ M<sub>23</sub>C<sub>6</sub> ในยูเท็กติกคาร์ไบด์มีแนวโน้มจะเข้าสู่ค่าคงที่ ซึ่งอาจเป็นสัดส่วนที่สมดุล ณ อุณหภูมินั้น ๆ
- 6. การปรับสภาพด้วยความร้อนเพิ่มความแข็งของบริเวณเดนไดรต์จากประมาณ 426 เป็นประมาณ 800 Hv (100gf/15s) และเพิ่มความแข็งโดยรวมจากประมาณ 510 เป็นประมาณ 770 Hv (30kgf/15s)
- สภาวะการปรับสภาพด้วยความร้อนที่เหมาะสมที่สุดในงานวิจัยนี้อยู่ที่ 1025 °C เป็นเวลา 4-6 ชั่วโมง แต่การสรุปที่แน่นอนยังต้องการการศึกษาเพิ่มเติมในแง่ปริมาณออสเตนในต์คงค้าง และคาร์บอนที่ เหลือละลายอยู่ในมาร์เทนไซต์หลังการปรับสภาพด้วยความร้อน
- 8. การศึกษาด้วยเทคนิค Electron Energy Loss Spectrometry พบว่า Near Edge Structure ของ C K-edge ในสเปกตรัมของ M<sub>7</sub>C<sub>3</sub> และ M<sub>23</sub>C<sub>6</sub> มีความแตกต่างกันอย่างเห็นได้ชัด ยืนยันศักยภาพของ เทคนิคนี้ในการวิเคราะห์ขนิดของคาร์ไบด์ ประกอบกับเทคนิคการเลี้ยวเบนของอิเล็กตรอน

- 2. ได้สร้างความร่วมมือกับกลุ่มวิจัยในต่างประเทศ ได้แก่ Dr. Andy Brown, Dr. R. Brydson และ Prof. D. V. Edmonds, Department of Materials, University of Leeds ประเทศจังกฤษ และได้ส่ง นักศึกษาปริญญาเอก (นางอัมพร เวียงมูล) ซึ่งทำวิจัยร่วมในโครงการเพื่อไปศึกษาเทคนิคต่างๆทาง จุลทรรศนศาสตร์อิเล็กตรอน ณ University of Leeds เป็นเวลา 1 ปี ในช่วงเดือนตุลาคม 2545ถึง เดือนกันยายน 2546
- 3. งานวิจัยได้สร้างความสนใจเทคนิคจุลทรรศนศาสตร์อิเล็กตรอนแบบส่องผ่านในงานโลหะวิทยาในวง กว้างขึ้น โดยเฉพาะแก่นักศึกษาบัณฑิตศึกษาสาขาวัสดุศาสตร์ และเริ่มมีนักศึกษาสมัครเข้าเรียน ปริญญาเอกโดยใช้เทคนิคนี้ในการศึกษาทางโลหะวิทยามากขึ้น

### ภาคผนวก

- ภาคผนวก 1 สำเนาบทคัดย่อผลงานวิจัยที่ได้นำเสนอในงานประชุมวิชาการระดับนานาชาติ จุลทรรศนศาสตร์อิเล็กตรอน อาเซียน ครั้งที่ 3 ณ โรงแรมปางสวนแก้ว จังหวัดเชียงใหม่ ระหว่างวันที่ 30 มกราคม ถึงวันที่ 1 กุมภาพันธ์ 2545 ภาคโปสเตอร์ และรางวัลต่าง ๆ
- ภาคผนวก 2 manuscript ผลงานที่ส่งตีพิมพ์ในวารสารวิชาการระดับนานาชาติ

  The International Journal of The Iron and Steel Institute of Japan (ISIJ)
  และสำเนาจดหมายจาก Editors
- ภาคผนวก 3 manuscript ผลงานที่ส่งนำเสนอในงานประชุมวิชาการระดับนานาชาติ
  The 8th Asian Foundry Congress ระหว่างวันที่ 13-14 ตุลาคม 2546
  ณ โรงแรมมีราเคิลแกรนด์ กรุงเทพมหานคร ภาคบรรยาย

### Poster Presentation

J.F.M.S.T. Vol.16 No.1, pp.177-178, 2002 Punted in Thailand

A. Wiengmoon<sup>1</sup>
T. Chairwangsri<sup>2</sup>
J.T.H. Pearce<sup>3</sup>

### Effects of Heat Treatment on Microstructure and Hardness of 30%Cr-2.4%C Cast Iron

Department of Physics, Faculty of Science, Chiang Mai University, Thaifand

Department of Industrial Chemistry, Faculty of Science, Chiang Mai University, Thailand

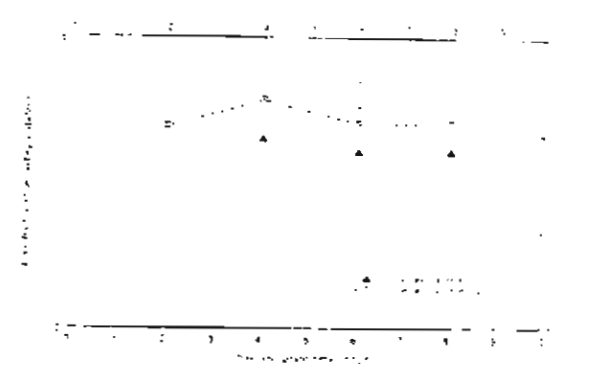
National Metal and Materials Technology Center, Bangkok 10400, Thailand

High chromium cast nons containing 30% Cr and 2.4% C are used for abrasion and corrosion resistance in wet wear applications. Their microstructure in the as cast condition consists of primary austenite dendrite, eutectic austenite (partly transformed to martensite) and eutectic carbides (M-C). The abrasion resistance and fracture toughness of these alloys depend on the type, morphology and distribution of the eutectic carbide and the supporting matrix. In some applications the austenite matrix has limited abrasion resistance but this can be improved by heat treatment to provide a martensite matrix. This heat treatment is called "destabilisation" and enables carbon and chromium in the austenite matrix to precipitate as secondary carbides. After cooling, the microstructure consequently consists of eutectic carbide (M<sub>2</sub>C<sub>3</sub>) and secondary carbides within a martensite matrix together with some retained austenite.

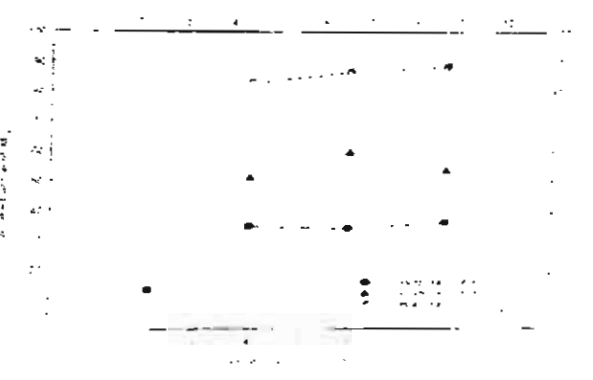
In this study, as east 30% (Cr - 2.4% (C east iron was destabilised in the temperature range of 900-1025. C for times of 2-8 hours, followed by air cooling to room temperature. Vickers macro-hardness and Vickers interohardness of the resultant martensite matrices were measured. Microstructures were studied by light inicroscopy and scanning electron microscopy (SEM). Volume fractions of secondary carbides and MaC<sub>6</sub> in eutectic carbides were determined from SEM micrographs. The distribution of secondary carbides was compared by measuring number per unit area of secondary carbides. Morphologies of secondary carbides were cube, discrete-rod or plate-like shapes (e.g. in Figure 1). A duplex structure was found in the eutectic carbides as shown in Figure 2. Higher destabilisation temperatures resulted in coarser secondary carbide structures with higher volume fractions (Figure 3) but reduced the number per unit area of secondary carbides (Figure 4). Longer destabilisation times in the range used in the experiment tended to increase the number per unit area of secondary carbides, but has no significant effect on their volume fraction. The volume fraction of  $M_{\rm Pl}C_{\rm b}$ within duplex structure of cutectic carbides was also increased as the destabilisation temperature and time were increased (Ligure 5). The results from macrohardness measurement (Figure 6) corresponded with the microstructural observations. At higher destabilisation temperature, the macrohardness was increased due to volume fraction of secondary carbides within matrix was increased. However, the maximum microhardness of the matrix was obtained at 950 C (Figure 7). The likely explanation is that lower destabilisation temperature give a fine distribution and higher number per unit area of secondary carbides, whereas for higher destabilisation temperature, the secondary earbides has bigger size and coarse distribution. This leads to reduction in microhardness. High destabilisation temperatures can also result in more retained austenite in air quenched structures which can contribute to lower measured hardness.



Figure 1 Morphology of secondary carbides (destabilised at 950 C for 6 hours).



**Figure 3** The effect of destabilisation on volume fraction of secondary earbide.



**Figure 5** The effect of destabilisation on volume fraction of  $M_{23}C_n$  carbide in the eutectic carbide.

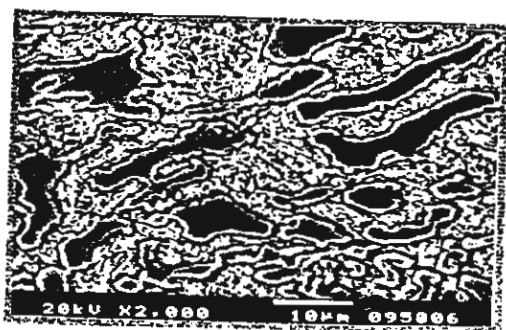


Figure 2 BEI showing the duplex of eutectic carbides (destabilised at 950°C for 6 hours).

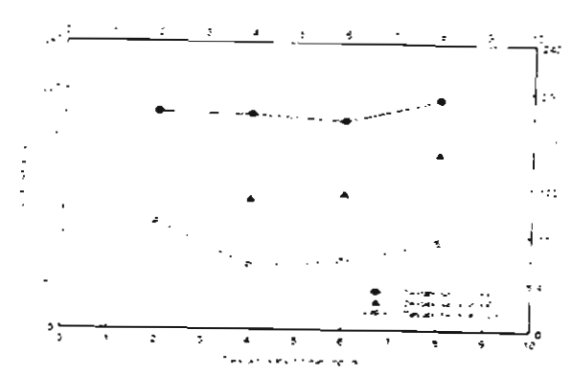
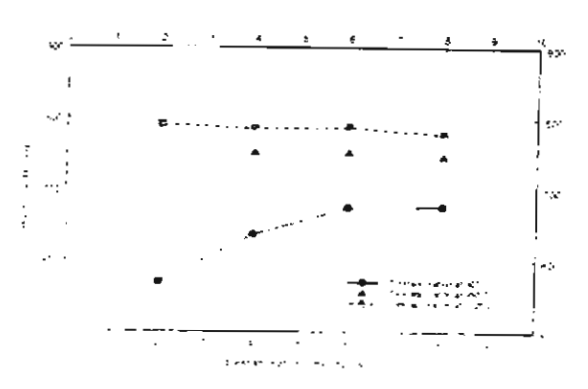


Figure 4 The effect of destabilisation on count per unit area of secondary carbide.



**Figure 6** The macrohardness of 30° <sub>n</sub>Cr irons in heat treated condition.

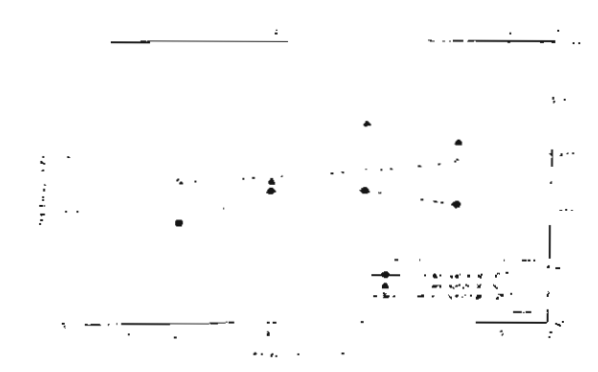


Figure 7 The microhardness of 30% Cr irons in heat treated condition.



## Microuradh Contact Nyara





Department of Physics, Faculty of Science, Chiang Mai University, Chiang Mai 50200, Thailand.

presented at

Conference of The Electron Microscopy Society of Thailand The 3rd ASEAN Microscopy Conference and The 19th Annual

January 30th - February 1st, 2002 The Lotus Pang Suan Kaew Hotel, Chiang Mai, Thailand

Framos Vanitanakom

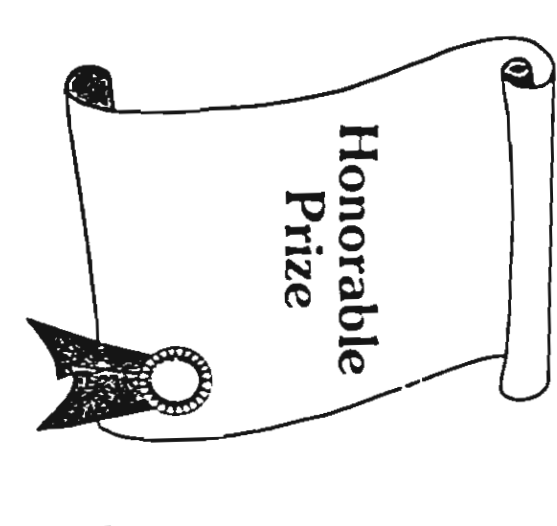
Chairperson of the Organising Committee

and Bythe

Chairperson of the Academic Affairs



# Micrograph Contest Award



### Materials Science: LM

A. Wiengmoon

Department of Physics, Faculty of Science, Chiang Mai University, Chiang Mai 50200, Thailand.

presented at

The 3rd ASEAN Microscopy Conference and The 19th Annual Conference of The Electron Microscopy Society of Thailand

January 30th - February 1st, 2002 The Lotus Pang Suan Kaew Hotel, Chiang Mai, Thailand

Promoto Vanittarakon.

Chairperson of the Organising Committee

Sur Bythin

Chairperson of the Academic Affairs











of 30%Cr-2.4%C Cast Iron **Effects of Heat Treatment on Microstructure and Hardness** 

A. Wiengmoon, T. Chairuangsri and J. T. H. Pearce

Prize

Sid

presented at

Conference of The Electron Microscopy Society of Thailand The 3rd ASEAN Microscopy Conference and The 19th Annual

January 30th - February 1st, 2002 The Lotus Pang Suan Kaew Hotel, Chiang Mai, Thailand

Pramoto Vanitanakon

and Orthor



Niikura Building (2F) 2 Kanda-Tsukasacho 2-chome, Chiyoda-ku, Tokyo 101-0048 JAPAN

Phone: +81-3-5209-7011

+81-3-5209-7012

+ 81-3-5209-7013

+ 81-3-5209-7014 Fax + 81-3-3257-1110

URL http://www.isij.or.jp.

0003

June 2, 2003

Dr.Torranin Chairuangsri
Faculty of Science
Department of Industrial Chemisry
Chiang Mai University
Chiang Mai 50200, Thailand

Dear Dr. Torranin Chairuangsri:

This is to acknowledge receipt of your paper titled "A microstructural study of destabilised 30wt%Cr-2.3wt%C high chromium cast iron" (Receipt No.:2003-343) for publication in *ISIJ International*. You will be advised in due course of the acceptability for publication in the journal.

With best regards.

Sincerely yours,

Shozo MIZOGUCHI

Editor-in-Chief.

Editorial Board of ISIJ International

(Professor, Tohoku University)

SM/TU/mh

### A Microstructural Study of Destabilised 30wt%Cr-2.3wt%C High Chromium Cast Iron

### A. WIENGMOON, T. CHAIRUANGSRI<sup>1)</sup> and J. T. H. PEARCE<sup>2)</sup>

Department of Physics, Faculty of Science, Chiang Mai University, 50200, Thailand.

1) Department of Industrial Chemistry, Faculty of Science, Chiang Mai University, 50200,

Thailand. E-mail: torra@chmai.loxinfo.co.th

2) National Metal and Materials Technology Center, Bangkok, 10400, Thailand.

### **SYNOPSIS**

An as-cast 30wt%Cr-2.3wt%C cast iron was destabilised in the temperature range of 900-1100 °C for times of 2-8 hours, followed by air cooling to room temperature. The resultant microstructures were examined using light microscopy (LM), scanning electron microscopy (SEM) and transmission electron microscopy (TEM). Volume fractions of secondary carbide within the martensite matrix and of M23C6 in eutectic carbides were determined. Vickers macrohardness and Vickers microhardness of the dendritic regions were also measured. It was found that morphologies of secondary carbide were cube, plate-like shape or discrete-rod. A duplex core-shell structure was found in the eutectic carbides after destabilisation. It consists of M<sub>7</sub>C<sub>3</sub> as a core surrounding by M<sub>23</sub>C<sub>6</sub>, while the secondary carbide in these alloys was identified as M<sub>23</sub>C<sub>6</sub>. Higher destabilisation temperatures resulted in coarser secondary carbides with comparable volume fraction, but less in counts per area. The volume fraction of M23C6 within the duplex structure was also increased when increasing destabilisation temperature and time. The results from hardness measurements revealed that the overall macrohardness of the iron was increased with increasing the destabilisation temperature up to about 770 HV(30kgf/15s) at 1,025 °C, whereas the microhardness of the dendritic regions reached the maximum value of 800 HV(100gf/15s) at about 1,025 °C.

KEY WORDS: high chromium cast iron; destabilisation; microstructure

1. INTRODUCTION 0002

High chromium cast irons are widely used as abrasion resistant materials in cement manufacturing, mineral processing and slurry pumping<sup>1-3)</sup>. Their high resistance to wear in these demanding situations stems from the presence of hard eutectic M<sub>7</sub>C<sub>3</sub> carbides in their microstructures. Most commercial alloys are based on hypo-eutectic compositions containing between 12 and 30wt%Cr and from 1-3wt%C plus additions of other elements such as Mo, Ni and Cu to improve hardenability. The most popular alloys, providing cost-effective solutions to wear problems in many applications, are based on Cr levels of 18-22wt%. Lower Cr irons containing around 12wt%Cr have lower initial costs but can only be used for less severe wear situations such as small grinding media. The 25-30wt%Cr alloys have been developed to provide resistance to the combined effects of abrasion and corrosion in wet grinding and in slurry transport. For all Cr irons, wear resistance, and mechanical properties in general, depend on the type, morphology and distribution of carbides, and on nature of the matrix structure<sup>4-9)</sup>.

The as-cast microstructure of the 25-30%Cr irons consists of primary austenite dendrites, eutectic austenite (partially transformed to martensite) and interdendritic eutectic M<sub>7</sub>C<sub>3</sub> carbide<sup>9)</sup>. The as cast irons posses useful resistance to abrasion under conditions which allow austenite to work harden<sup>10)</sup> but have limited fracture toughness. Improved service performance can be obtained by heat treatments and additional alloying to provide harder, more wear resistant martensitic matrix structures or to obtain austenitic matrices with improved crack propagation resistance<sup>2,4,6-8)</sup>.

Conventional heat treatment involves heating castings to and holding at 950-1050°C, followed by air hardening and tempering. The holding period is called "destabilisation", since it allows carbon and chromium in the austenite matrix to come out of solution as precipitates of secondary carbide<sup>9,11-12)</sup>. This lowers the alloy content of the austenite, raising the M<sub>S</sub> temperature and thus enables the austenite to transform to martensite on forced air-cooling. The

resultant microstructure consists of eutectic carbide (M<sub>7</sub>C<sub>3</sub>) and secondary carbides within a martensite matrix together with some retained austenite. Single, or sometimes double, tempering treatments are then used to temper the martensite and to reduce the amount of the residual austenite<sup>12</sup>.

The nature of secondary carbide formation has been the subject of several studies <sup>[1-17]</sup>. It has been shown that the secondary carbides do not nucleate and grow on the eutectic carbides but form separately within the original dendritic regions <sup>[1-13]</sup>. The secondary carbides in 15-20% Cr irons have been identified as M<sub>7</sub>C<sub>3</sub> and as M<sub>23</sub>C<sub>6</sub> in 25-30%Cr irons <sup>[3,13-15]</sup>. Destabilisation treatments do not appear to have any significant effects on the form of the eutectic carbides in irons containing up to about 28%Cr. However at the 30%Cr level destabilisation treatments do affect the eutectic M<sub>7</sub>C<sub>3</sub> carbide, causing it to partially transform to M<sub>23</sub>C<sub>6</sub> carbide. Under TEM examination this M<sub>23</sub>C<sub>6</sub> carbide can be recognised as shells surrounding the M<sub>7</sub>C<sub>3</sub> cores. Unlike the highly faulted M<sub>7</sub>C<sub>3</sub>, the M<sub>23</sub>C<sub>6</sub> is free from stacking faults but does contain dislocation networks and grain boundaries <sup>[3,16,18)</sup>. This structural change in the eutectic carbides could be part of the reason for an observed lack of improvement in high stress abrasion resistance of 30% Cr iron after a conventional hardening heat treatment in which the micro-hardness of the dendritic regions was increased to 800 HV compared to 500 in the as-cast condition, but the wear abrasion resistance did not improve<sup>2)</sup>.

Although some TEM characterisation of 30%Cr irons had been performed during previous work<sup>3,13,18</sup>, no attention was given to the effects of heat treatment variables on the M<sub>7</sub>C<sub>3</sub> to M<sub>23</sub>C<sub>6</sub> transition in the eutectic carbides. Hence the objective of the present work is to study how variations in destabilisation temperatures and times can influence this transformation and other microstructural aspects of a 30% Cr cast iron.

### 2 MATERIALS AND METHODS

### 2.1. Materials Preparation and Heat Treatment

A 30wt%Cr-2.3wt%C high chromium cast iron was prepared by melting a charge based on low Si pig iron and ferroalloys in an induction furnace. The molten iron was cast at a pouring temperature of 1500 °C into a CO<sub>2</sub> silicate sand mould as cylindrical bars with a diameter of 2.50 cm. The chemical composition of the as-cast alloy is shown in Table 1. The bars were then sectioned as specimens with a thickness of about 1.50 cm. These as-cast specimens were heat treated (destabilised) in a muffle furnace at the temperature range of 900-1100 °C for times of 2-8 hours, followed by cooling to room temperature in still air. A controlled atmosphere was not used.

(Please insert Table 1 here.)

### 2.2. Sample Preparation for Microstructural Investigation

Specimens for light microscopy (LM) and scanning electron microscopy (SEM) were ground on silicon carbide papers down to 1,000 grits and then polished with 6, 3 and 1 µm diamond paste. The etchants used were (i) Murakami's reagent, containing 10 g potassium ferricyanide and 10 g potassium hydroxide in 100 ml distilled water and (ii) 4 g potassium permanganate and 4 g sodium hydroxide in 100 ml distilled water. The microstructure was studied using an Olympus BX60M optical microscope and a JSM-5410LV scanning electron microscope equipped with secondary and back-scattered electron detectors. The scanning electron microscope was operated at 20 kV and a working distance of 14 mm from the objective lens pole piece. Thin foils for transmission electron microscopy (TEM) were prepared by sectioning heat treated specimens, perpendicular to the axis of the as-cast cylindrical rod, by a CBN saw to obtain thin slices with thickness of about 200 µm. Both sides of the slices were then ground manually on silicon carbide papers down to 1,200 grits to reduce the thickness to about 80-100 µm. 3 mm discs were punched out and then thinning by a Struer. Tenupol-3 twin-jet

electropolisher operated at 20-26 V, 22 °C and approximately 0.1 A, using 10 vol% perchloric acid in acetic acid as an electrolyte. Thin foils were examined by a JEOL JEM-1200EXII transmission electron microscope operating at 100 kV. Fig. 1 schematically illustrates the sample preparation procedure for LM, SEM and TEM.

(Please insert Fig. 1 here.)

### 2.3. Quantitative Metallography

The volume fraction of the secondary carbide within the matrix was determined by point counting choosing only those particles which were greater than 0.2  $\mu$ m. To obtain this information, an intercept plan was superimposed on the enlarged SEM micrographs. The spacing distance of the plan is equivalent to 0.3  $\mu$ m. The mean value is based on ten different areas.

The distribution of the secondary carbide was compared by measuring counts per area (Cs/100  $\mu$ m<sup>2</sup>) of secondary carbide particles. The area was calculated from the micron bar on SEM micrographs. Only the particles which are greater than 0.1  $\mu$ m were counted. The mean value is based on ten different areas.

The mean value of the volume fraction of M<sub>23</sub>C<sub>6</sub> in duplex structure of eutectic carbides was also determined from SEM micrographs using the same procedure.

### 2.4. Hardness Measurement

The specimens prepared for LM and SEM were also used for the hardness measurements. Vickers microhardness of the dendritic regions was measured on etched specimens using 100 gf load and 15 seconds indenting time. The mean values are based on twelve different indentations. A Galileo microhardness tester was utilised in this experiment. Vickers macrohardness testing was performed on non-etched specimens using 30 kgf load and

15 seconds indenting time. The mean value are based on sixteen different indentations. A Brooks hardness tester was used in this experiment.

### 3. RESULTS AND DISCUSSION

### 3.1. General Observation on Microstructure

The microstructure in the as-cast condition consists of primary austenite ( $\gamma$ ) dendrites with a eutectic structure (eutectic austenite partially transformed to martensite and eutectic  $M_7C_3$  carbide) as shown in Fig. 2. After destabilisation heat treatment, as shown in Fig. 3, the microstructure of the iron consists of precipitated secondary carbides within a martensite matrix and possibly some retained austenite, together with eutectic  $M_7C_3$  carbide partially transformed to  $M_{23}C_6$ .

(Please insert Fig. 2 here.)

(Please insert Fig. 3 here.)

The morphologies of secondary carbides illustrated in Fig. 4 are cube, discrete-rod or plate-like shapes. The secondary carbide particles in the region close to the eutectic carbides are apparently smaller than in the region far away from the eutectic carbides. This precipitation characteristic can be attributed to the segregation of carbon and chromium to the outer regions of the dendrites as they grew during solidification<sup>15,19)</sup>. Higher destabilisation temperatures resulted in coarser particles as seen in Fig. 5.

(Please insert Fig. 4 here.)

(Please insert Fig. 5 here.)

After destabilisation, a duplex structure was found in the eutectic carbides. It is thought that a thermodynamically more stable  $M_{23}C_6$  replaced the metastable  $M_7C_3$  carbide during destabilisation heat treatment. Therefore, the duplex carbides consist of  $M_{23}C_6$  shells surrounding eutectic  $M_7C_3$  cores as clearly seen under backscattered electron mode in Fig. 6. At

a particular destabilisation time, the magnitude of transition from M<sub>7</sub>C<sub>3</sub> to M<sub>23</sub>C<sub>6</sub> in eutectic carbides was increased as the destabilisation temperature was increased. This can be seen in Fig. 7 where the outer regions of eutectic carbides, i.e. M<sub>23</sub>C<sub>6</sub> were preferentially etched out by the etchant, leaving islands of eutectic M<sub>7</sub>C<sub>3</sub> as cores. It should be noted that the etchant in this case, which is 4 g potassium permanganate and 4 g sodium hydroxide in 100 ml distilled water, is superior than Murakami's reagent in revealing such a duplex structure.

(Please insert Fig. 6 here.)

(Please insert Fig. 7 here.)

### 3.2. TEM Examination

Results from TEM examination revealed that the dendritic matrix after destabilisation is martensite ( $\alpha'$ ). The results confirmed the duplex core-shell structure of the eutectic carbides formed after destabilisation, as shown in Fig. 8. The two carbides are clearly distinguished since faulting contrast is observed only in the  $M_7C_3$ . Pearce<sup>9.18)</sup> reported that this contrast in the hexagonal  $M_7C_3$  is believed to result from the presence of stacking faults or twins.

(Please insert Fig. 8 here.)

Secondary carbides precipitated within martensite matrix are shown in Fig. 9. The corresponding selected area diffraction pattern confirms that they are M<sub>23</sub>C<sub>6</sub> as reported previously<sup>18</sup>. It has also been reported<sup>3,15</sup> that secondary carbide does not precipitate on the eutectic carbides but formed preferentially within the dendritic matrix and this is again confirmed by the TEM investigation in this study. A doubt could then been asked why such a heterogeneous site as eutectic carbide/dendritic primary austenite interphase boundaries did not act as a preferential site for secondary M<sub>23</sub>C<sub>6</sub> carbide. The likely explanation is two folds. Firstly, the formation of the M<sub>23</sub>C<sub>6</sub> carbide as a shell of M<sub>7</sub>C<sub>3</sub> carbide along the eutectic structure is perhaps a peritectoid type consuming both M<sub>7</sub>C<sub>3</sub> and the adjacent austenite matrix. Secondly, the formation of the M<sub>23</sub>C<sub>6</sub> may not only a result from the M<sub>7</sub>C<sub>3</sub>-M<sub>23</sub>C<sub>6</sub> transformation alone,

but also from the secondary precipitation from the adjacent austenite matrix. After nucleation, probably on  $M_7C_3$ , those grains of  $M_{23}C_6$  carbide shell should be able to grow also into the dendritic primary austenite during the destabilisation heat treatment by diffusional growth and elements i.e. Cr and C could be conveyed between the  $M_{23}C_6$  shell and the dendritic austenite via. interphase boundary diffusion or even volume diffusion. Schematic illustration of the formation of  $M_{23}C_6$  is given in Fig. 10. The moving interphase boundary as such is therefore not a preferential site for nucleation of a new grain of secondary  $M_{23}C_6$  carbide. However, more evidence is needed before any conclusion can be drawn.

(Please insert Fig. 9 here.)

(Please insert Fig. 10 here.)

### 3.3. Quantitative Metallography

Effects of destabilisation conditions on the volume fraction of secondary carbides were shown in Fig. 11(a). The volume fraction of secondary carbide formed after destabilisation conditions used in this experiment is in the range of about 10-20 vol%. The deviation of the volume fraction of secondary carbides at different destabilisation conditions was within the error limit. Therefore, destabilisation temperatures and times in the range used in this experiment have seemingly no significant effect on the volume fraction of the secondary carbide.

The distribution of secondary carbide was compared by measuring number per area of secondary carbides. Higher destabilisation temperatures reduced the number per area of secondary carbides. For example, the counts per 100 µm² at 900 °C is about a factor of three compared to that at 1,025 °C. This can be attributed to the thermodynamic effect on enhancing nucleation rate at lower destabilisation temperature. The results are also in agreement with the microstructural examination shown in Fig. 5, where, at higher destabilisation temperature, coarser secondary carbide particles and their agglomerate were observed preferentially on heterogeneous sites. Even it is not clear, longer destabilisation times at the destabilisation

temperature up to 950 °C tend to increase the number per area of secondary carbides, as can be seen in Fig. 11(b). However, at higher destabilisation temperatures, the reverse effect is observed and this could result from coarsening or Ostwald ripening of the secondary carbide particles.

From Fig. 11(c), the volume fraction of  $M_{23}C_6$  within the duplex structure of eutectic carbides in this experiment is in the range of 20-99 vol%. It was increased as the destabilisation temperature and time were increased and, at a longer destabilisation time, tended to reach a limited value which could possibly be close to the equilibrium value at a particular temperature.

### 3.4. Overall Macrohardness and Microhardness of the Dendritic Region

Fig. 12(a) and 12(b) illustrate the microhardness within the dendritic regions and the overall macrohardness as a function of time and temperature of destabilisation, respectively. The hardness values of the as cast iron are also shown. Destabilisation heat treatment of this iron increased the microhardness of the dendritic regions from about 426 up to about 800 HV (100gf/15s) and the overall macrohardness from about 510 up to about 770 HV(30kgf/15s). This is comparable to what has been reported previously2). The macrohardness was increased as the destabilisation temperature increased up to 1,025 °C, while the microhardness of the dendritic regions reached the maximum value at 1,025 °C for 4-6 hours. This behaviour is complicated because many factors get involved including volume fraction of secondary carbide, their distribution, the different properties of martensite formed, and the amount of the retained austenite at a particular temperature. Precipitation of the secondary carbide is a hardening effect for the dendritic regions. However, this factor have to counteract with others leading to softening effects for the dendritic regions e.g. the softer martensite when it is less in carbon due to the higher volume fraction of secondary carbides precipitated, and possibly the more retained austenite in air quenched structures at high destabilisation temperatures<sup>3)</sup>. The compensation between these factors could result in an optimum destabilisation condition giving the maximum

macrohardness of the dendritic regions at 1,025 °C. The explanation for the overall macrohardness is even more difficult since we needs to take also the structure and properties of the eutectic carbides into account. The results suggest that the formation of duplex core-shell structure of eutectic carbides with higher volume fraction of the M<sub>23</sub>C<sub>6</sub> shell could also act as another softening factor for the destabilised 30wt%Cr-2.3wt%C iron, because the overall macrohardness at a particular condition is generally lower than that of the microhardness of the dendritic matrix, especially at higher destabilisation temperature with higher magnitude of M<sub>7</sub>C<sub>3</sub>-to-M<sub>23</sub>C<sub>6</sub> transformation. Further study should be carried out on quantifying the amount of retained austenite and of dissolved carbon within the martensite matrix.

(Please insert Fig. 11 here.)

(Please insert Fig. 12 here.)

4. CONCLUSIONS 0002

(1) Destabilisation heat treatment of a 30wt%Cr-2.3wt%C high chromium cast iron in the temperature range of 900-1100 °C for 2-8 hours led to precipitation of secondary M<sub>23</sub>C<sub>6</sub> carbide with the volume fraction and the number per area in the range of 10-20 vol% and 30-200 Cs/100 μm<sup>2</sup>, respectively.

- (2) Higher destabilisation temperatures resulted in coarser secondary carbide precipitated preferentially at heterogeneous sites with comparable volume fraction, but lesser number per area.
- (3) M<sub>7</sub>C<sub>3</sub> eutectic carbide transformed to M<sub>23</sub>C<sub>6</sub> carbide during destabilisation heat treatment forming a core-shell structure. The volume fraction of M<sub>23</sub>C<sub>6</sub> shell is in the range of 20-99 vol%, increasing with destabilisation temperature and time. Formation of this M<sub>23</sub>C<sub>6</sub> shell is believed to be either a peritectoid type or a result of not only the M<sub>7</sub>C<sub>3</sub>-to-M<sub>23</sub>C<sub>6</sub> transformation, but also the secondary precipitation from dendritic primary austenite.
- (4) Destabilisation heat treatment raised the microhardness of the dendritic regions from the ascast condition of about 426 up to about 800 HV(100gf/15s). The maximum microhardness of the dendritic regions was obtained at 1,025 °C with the value of 800 HV(100gf/15s).
- (5) Destabilisation heat treatment conditions used in this experiment increased the overall macrohardness of the 30wt%Cr-2.3wt%C iron from the as-cast condition of about 510 up to about 770 HV(30kgf/15s).

### **ACKNOWLEDGEMENTS**

Biotechnology Center, Mae-Jo University, Center of Instrumental Analysis, Suranaree University and Electron Microscopy Unit, Faculty of Medicine, Chiang Mai University are thanked for electron microscopy facilities. The authors would also like to thank The Thailand Research Fund (TRF) for funding support of this work.

### REFERENCES

- 1) R. W. Durman: International Journal of Mineral Processing, 22 (1988), 381.
- 2) J. T. H. Pearce: British Foundryman 78, (1985), 13.
- 3) J. T. H. Pearce: The Foundryman 95, (2002), 156.
- 4) M. Fiset, K. Peev and M. Radulovic: Journal of Materials Science Letters, 12 (1993), 615.
- 5) K. Peev, M. Radulovic and M. Fiset: Journal of Materials Science Letters, 13 (1994), 112.
- 6) M. Radulovic, M. Fiset and K. Peev: Journal of Materials Science, 29 (1994), 5085.
- 7) C. P. Tabrett: International Materials Reviews, 41 (1996), 59.
- 8) S. K. Hann and J. D. Gates: Journal of Materials Science, 32 (1997), 1249.
- 9) J. T. H. Pearce: AFS Transaction, 92 (1984), 599.
- 10) J. T. H. Pearce: Wear. 89 (1983), 333.
- 11) G. L. F. Powell and G. Laird: Journal of Materials Science, 27 (1992), 29.
- 12) J. T. H. Pearce and D. W. J. Elwell: Proceedings of Best Practices in the Production, Processing and Thermal Treatment of Castings, Raffles City Convention Centre, Singapore, 10-12 October, (1995), 26-1 to 18.
- 13) J. T. H. Pearce: Proceedings of Solidification Science and Processing: Outlook for the 21<sup>st</sup> Century, Bangalore, India, Edited by: B. K. Dhindaw, B. S. Murty and S. Sen, Oxford & IBH Publishing, New Delhi, ISBN 81-204-1514-0, 18-21 February, (2001), 241.
- 14) K.A. Kibble and J. T. H. Pearce: Cast Metals, 6 (1993), 9.
- 15) K. A. Kibble and J. T. H. Pearce: Cast Metals, 8 (1995), 123.
- 16) J. D. B. Demello, M. D. Charr and S. H. Thibault: Metallurgical Transactions A, 14A (1983), 1793.
- 17) A. Inoue and T. Masumoto: Metallurgical Transactions A, 11A (1980), 739.
- 18) J. T. H. Pearce and D. W. L. Elwell: Journal of Materials Science Letters, 5 (1986), 1063.
- 19) P. Dupin, J. Saverna and J. M. Schissler: AFS Transactions, 90 (1982), 711.

Table 1. Chemical composition of the high chromium cast iron.

Element	С	Cr	Si	Mn	S	P	Ni	Cu	Мо	Al
(wt%)	2.26	29.98	0.52	0.30	0.013	0.025	0.30	0.02	0.08	0.009

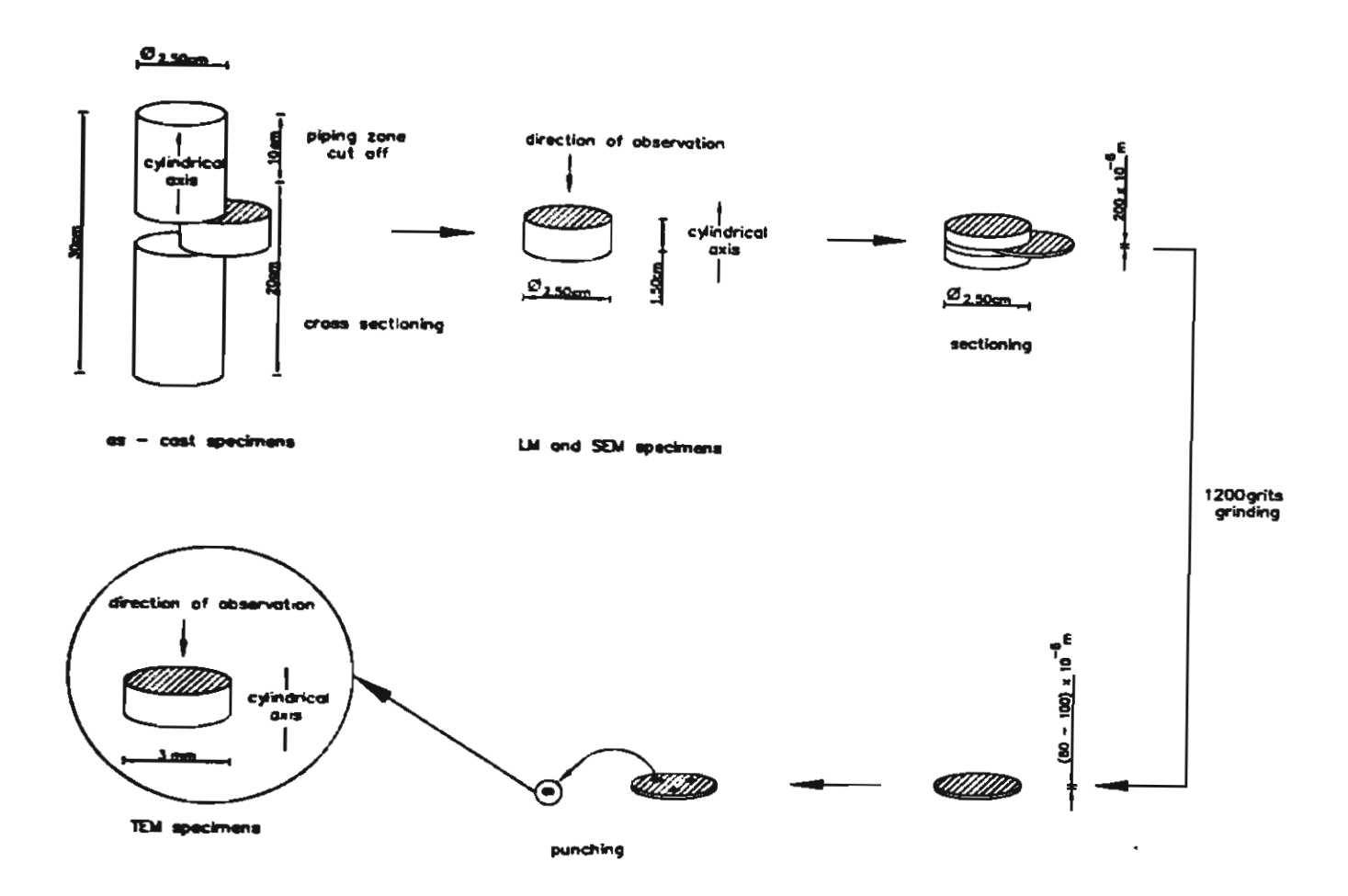
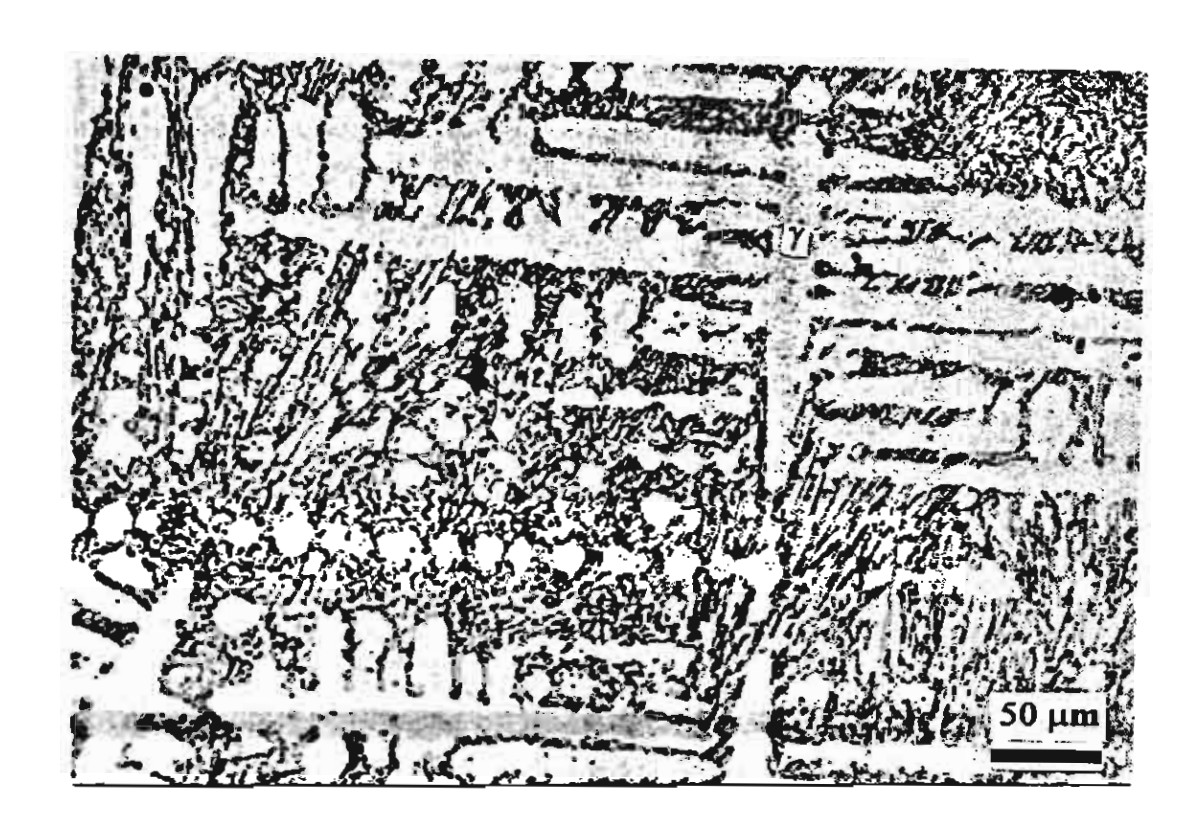


Fig. 1. Sample preparation procedure for LM, SEM and TEM.



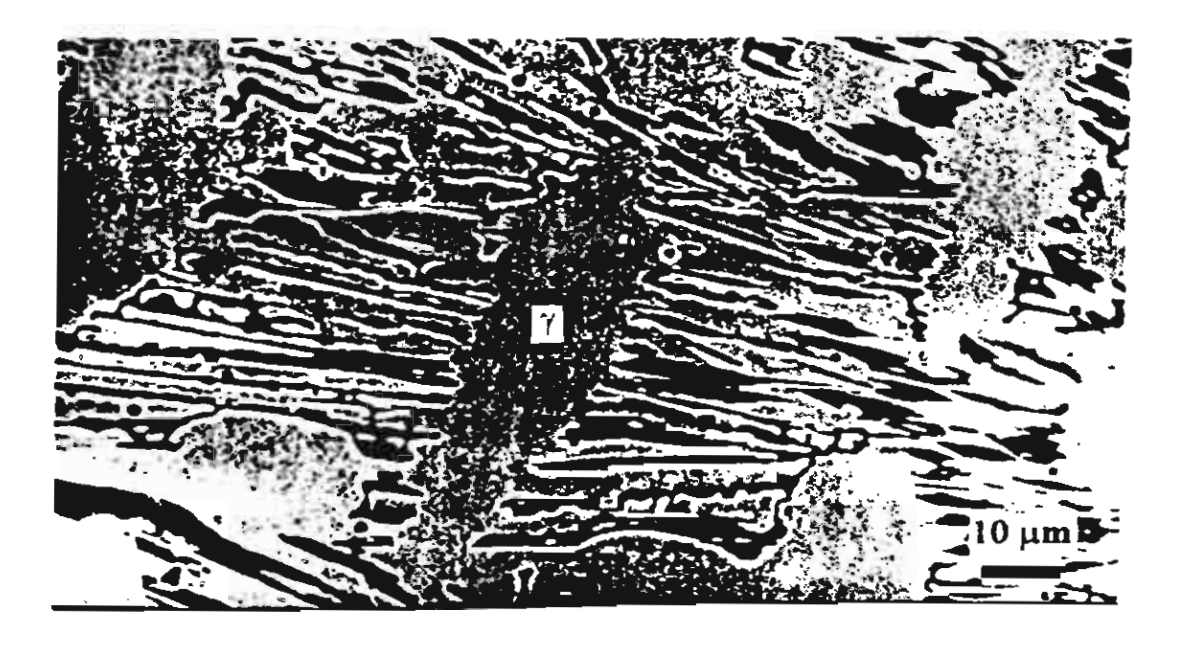
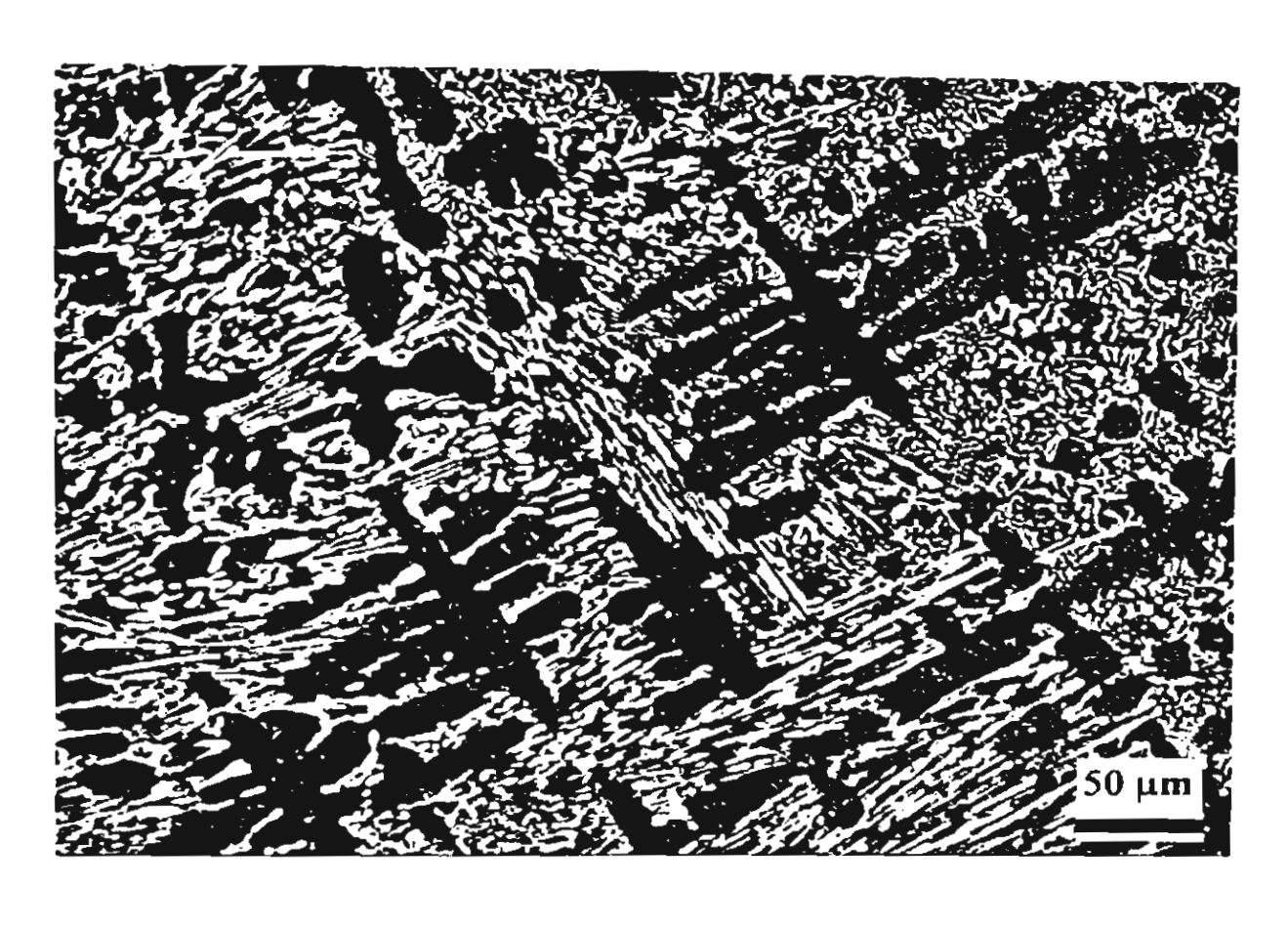
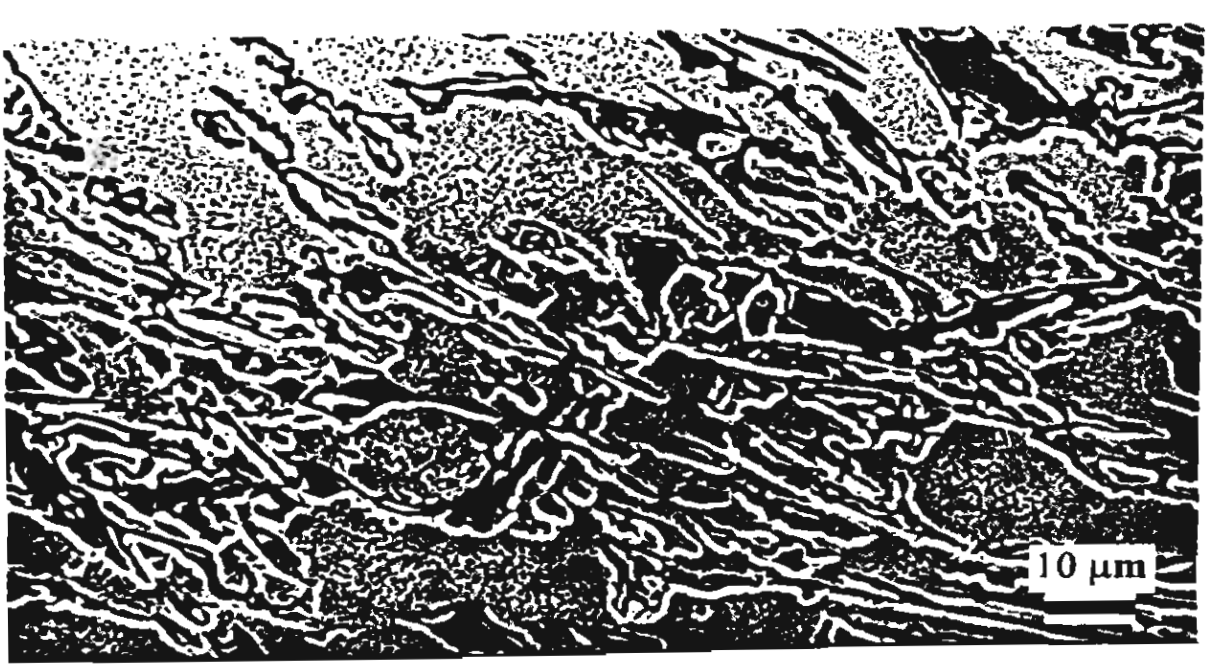
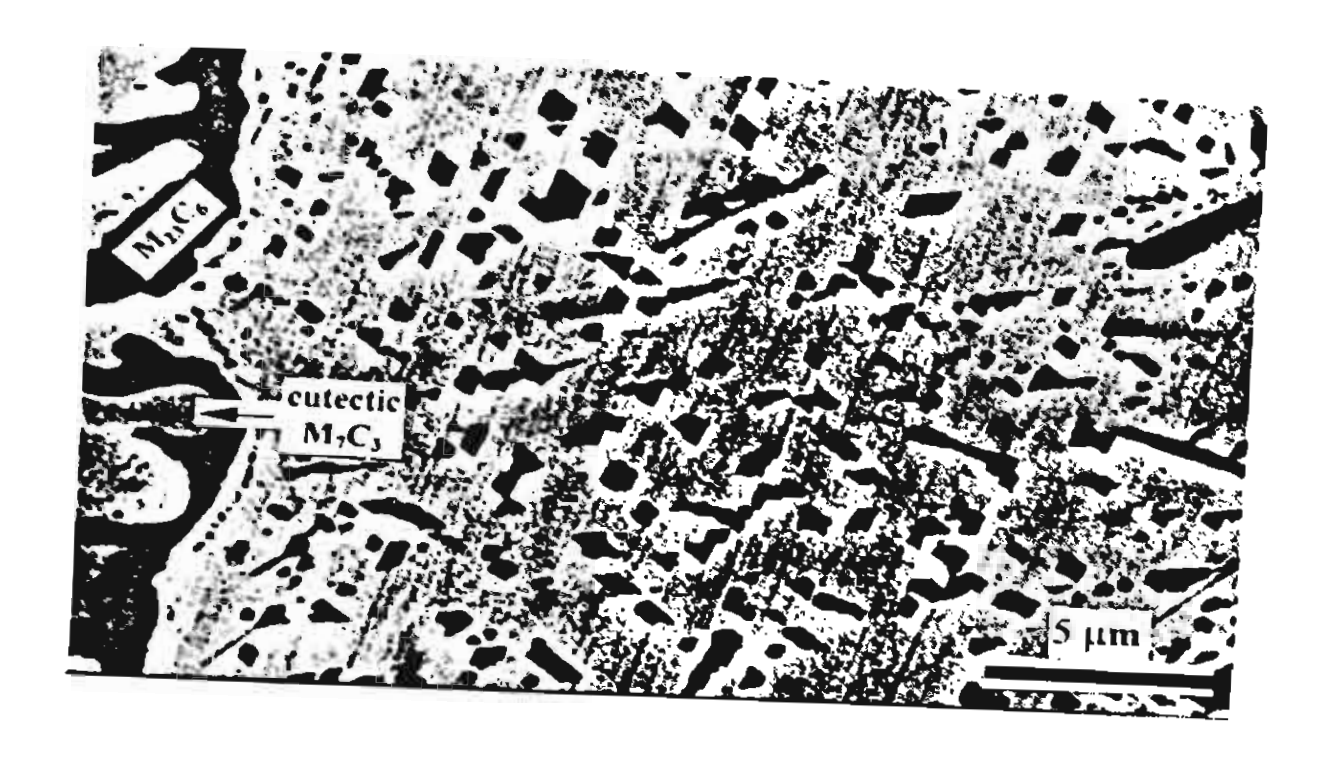


Fig. 2. Typical microstructure of the as-cast condition. γ denotes the dendritic austenite.
(a) LM (b) SEM (Etchant : 4 g potassium permanganate and 4 g sodium hydroxide in 100 ml distilled water)



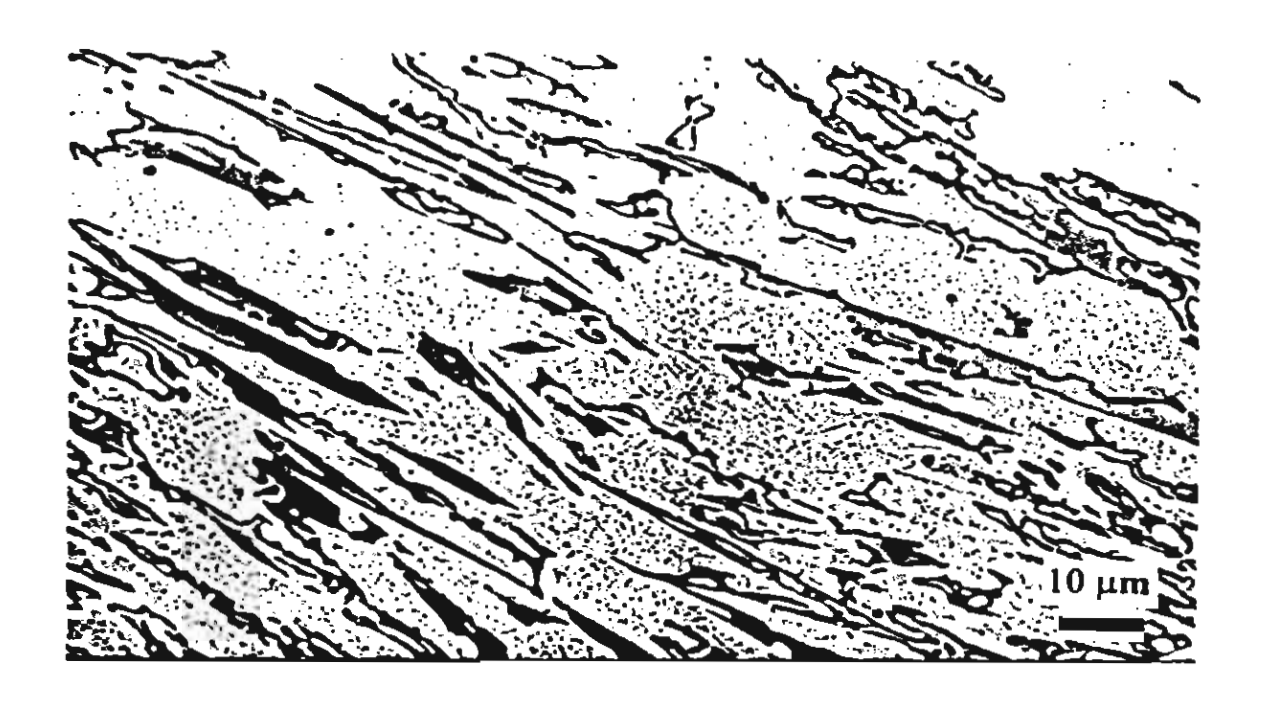


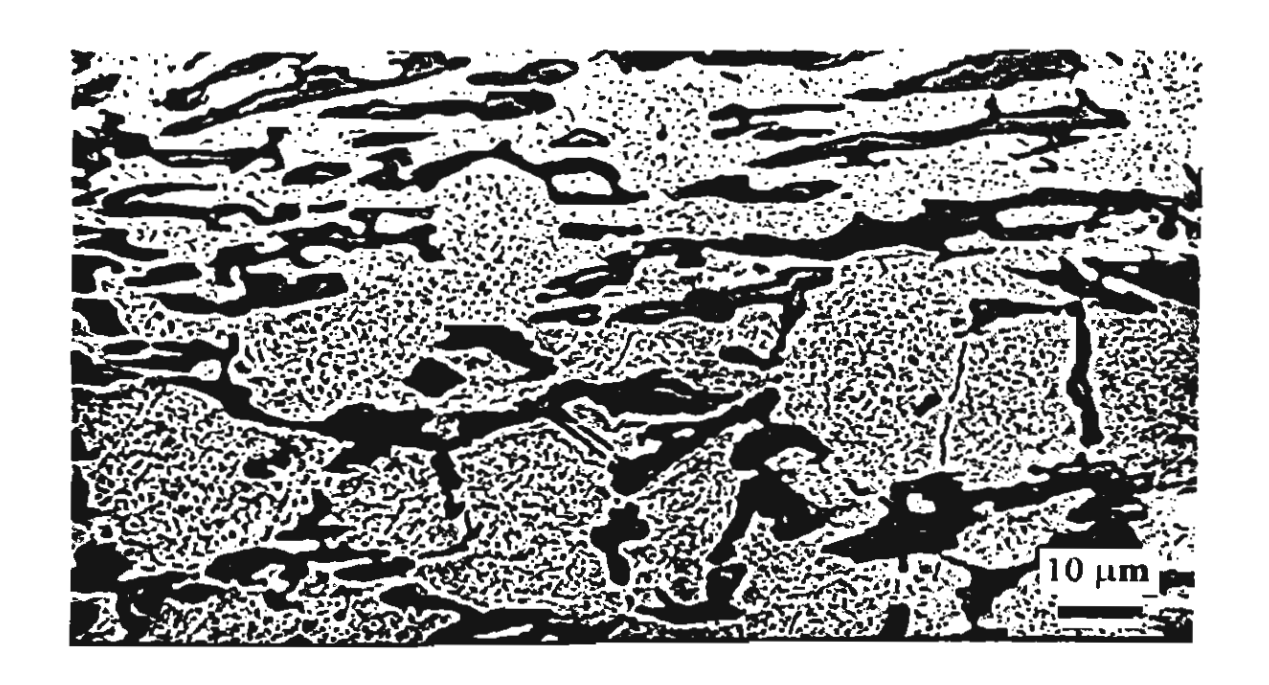
Typical microstructure after destabilisation heat treatment. (950 °C for 8 hours). Fig. 3. (a) LM (Etchant : Murakami's reagent) (b) SEM (Etchant : 4 g potassium permanganate and 4 g sodium hydroxide in 100 ml distilled water)

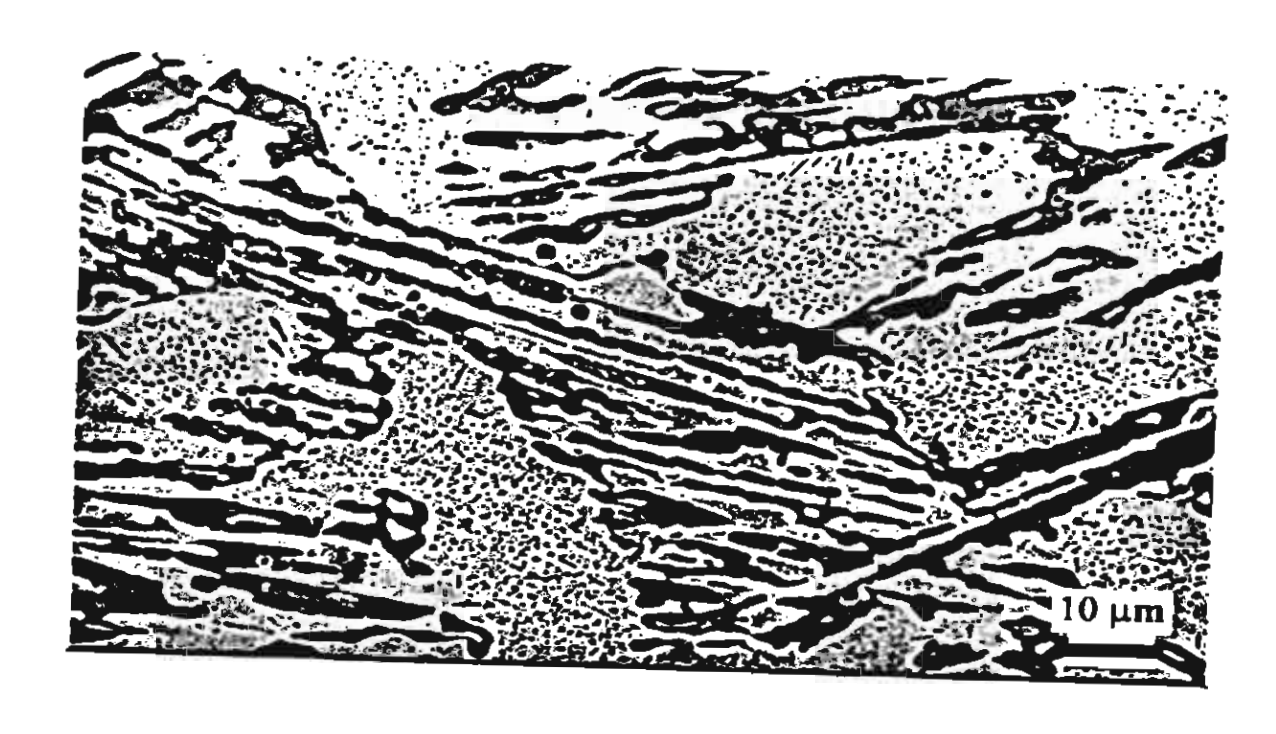




**Fig. 4.** Secondary electron images show morphologies of secondary carbide after destabilisation. (a) 4 hours at 950 °C and (b) 6 hours at 1025 °C. (Etchant : 4 g potassium permanganate and 4 g sodium hydroxide in 100 ml distilled water)







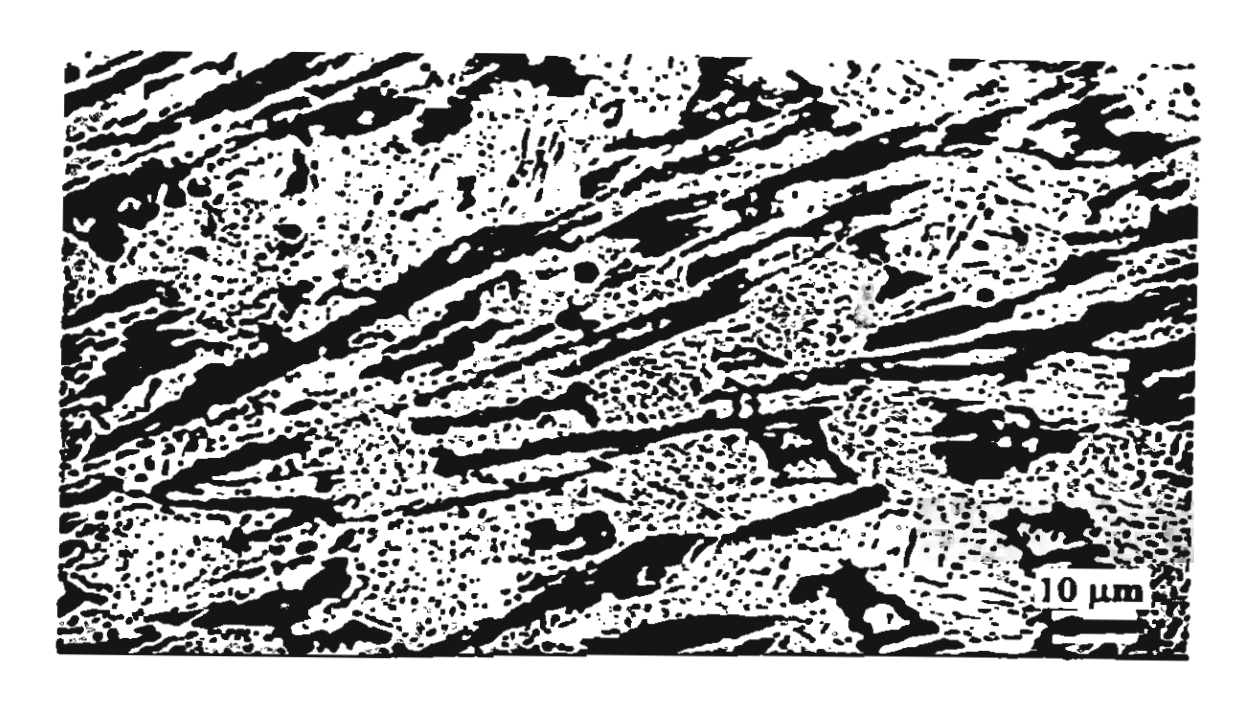


Fig. 5. Secondary electron images show the effect of destabilisation temperature on size and distribution of secondary carbide; destabilisation at 900 °C (a), 950 °C (b), 1025 °C (c) and 1100 °C (d). Holding time is 4 hours for all. (Etchant : 4 g potassium permanganate and 4 g sodium hydroxide in 100 ml distilled water)

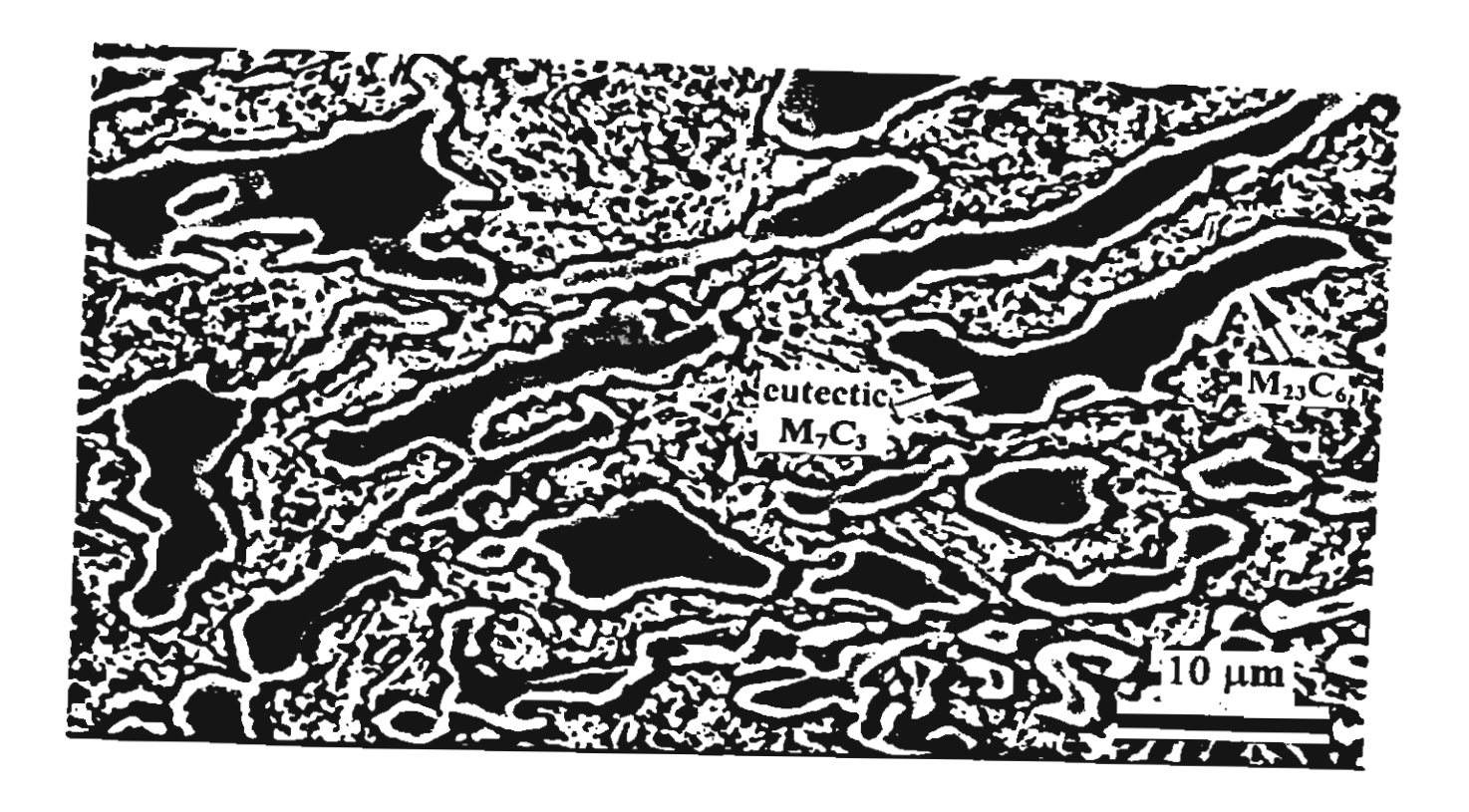
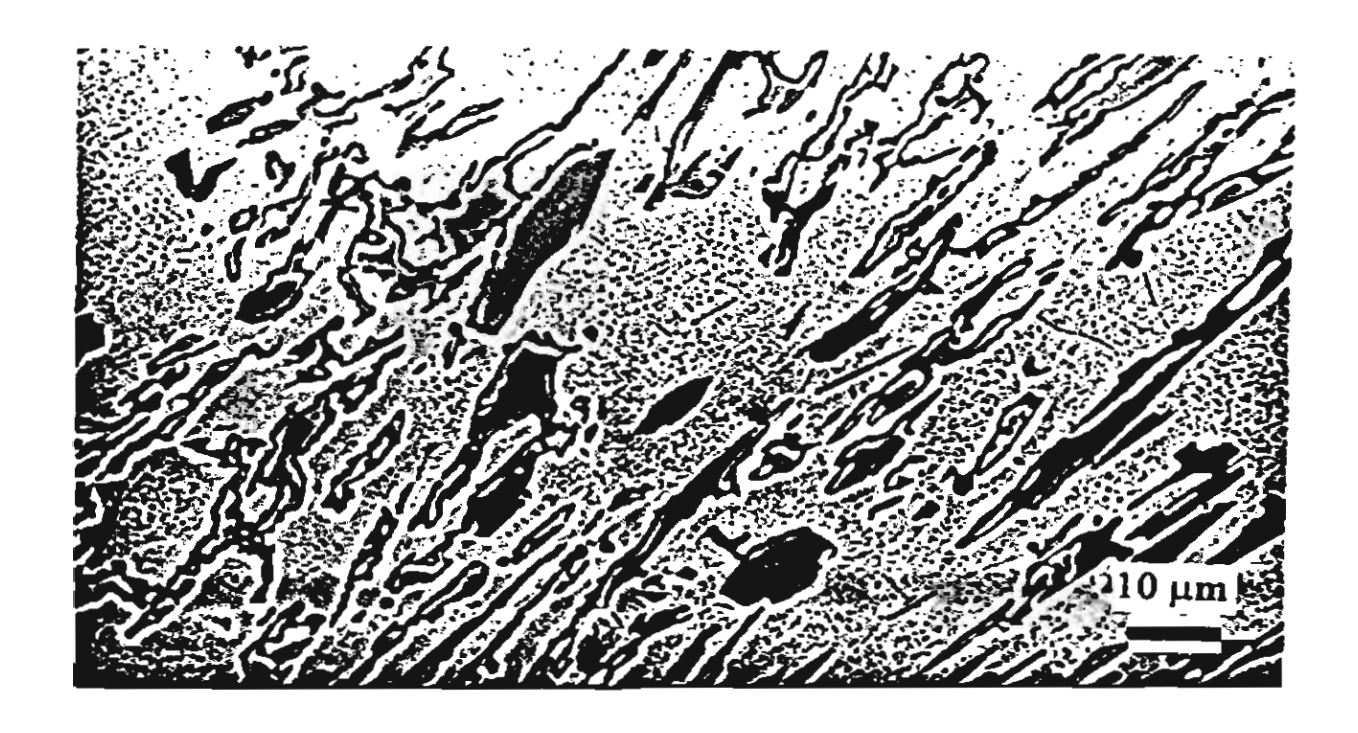
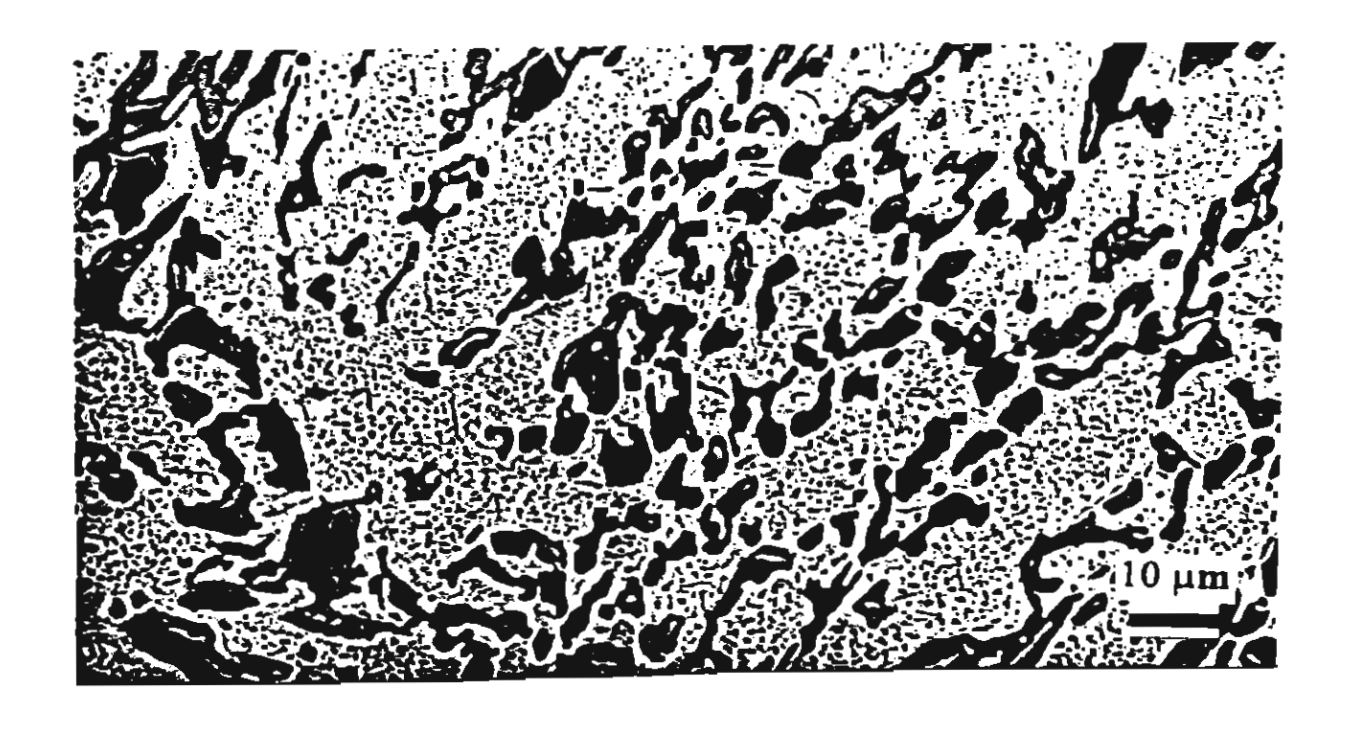
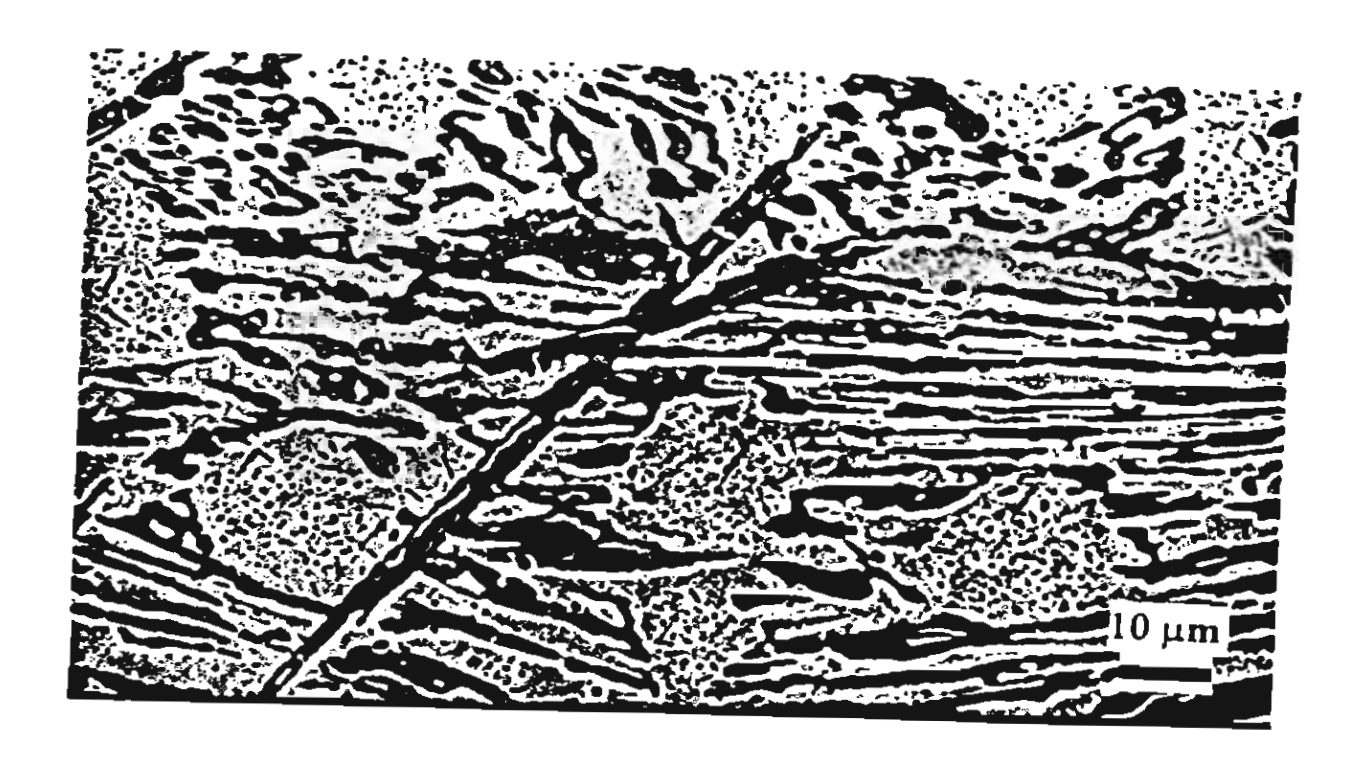


Fig. 6. Backscattered electron image shows the duplex structure of eutectic carbides (6 hours, 950 °C). The outer shell with brighter contrast is  $M_{23}C_6$ , while the core is eutectic  $M_7C_3$ . (Etchant: Murakami's reagent)







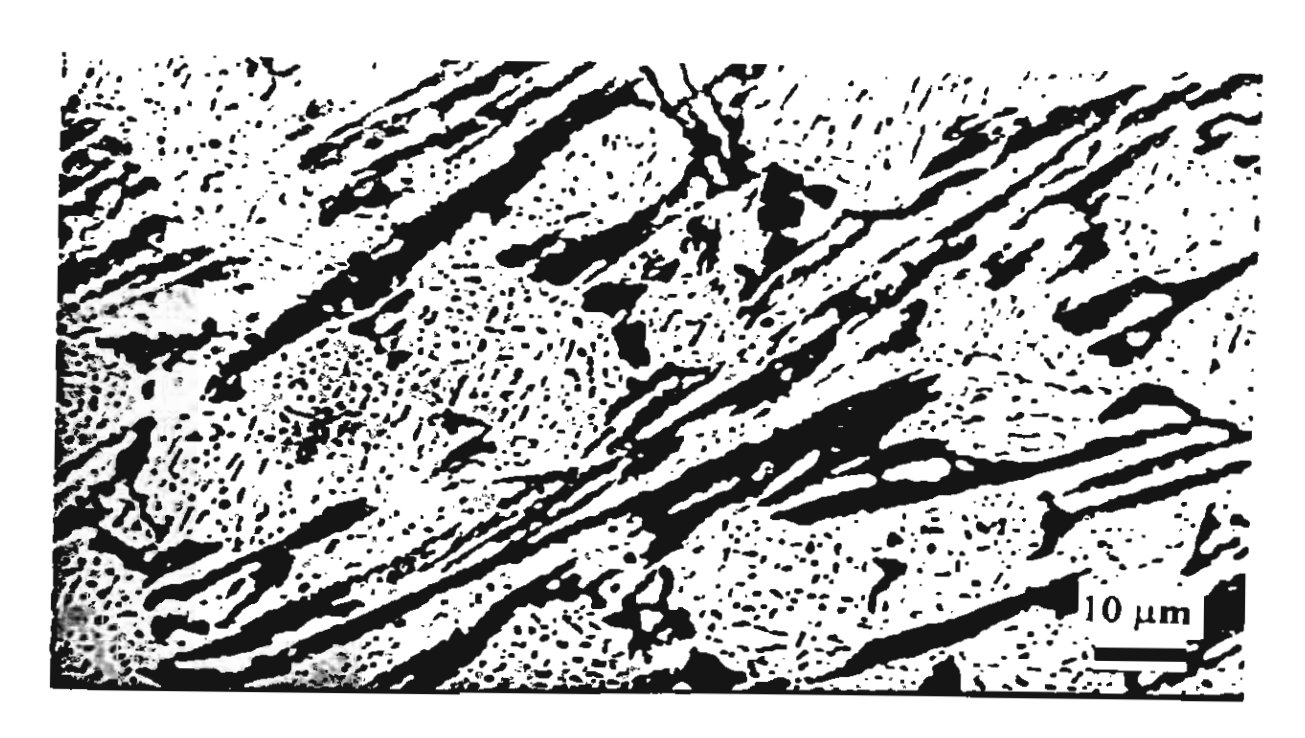


Fig. 7. Secondary electron images show the effect of destabilisation temperature on the magnitude of transition from M<sub>7</sub>C<sub>3</sub> to M<sub>23</sub>C<sub>6</sub> (preferentially etched out); destabilisation at 900 °C (a), 950 °C (b), 1025 °C (c) and 1100 °C (d). Holding time is 8 hours for all. (Etchant : 4 g potassium permanganate and 4 g sodium hydroxide in 100 ml distilled water)

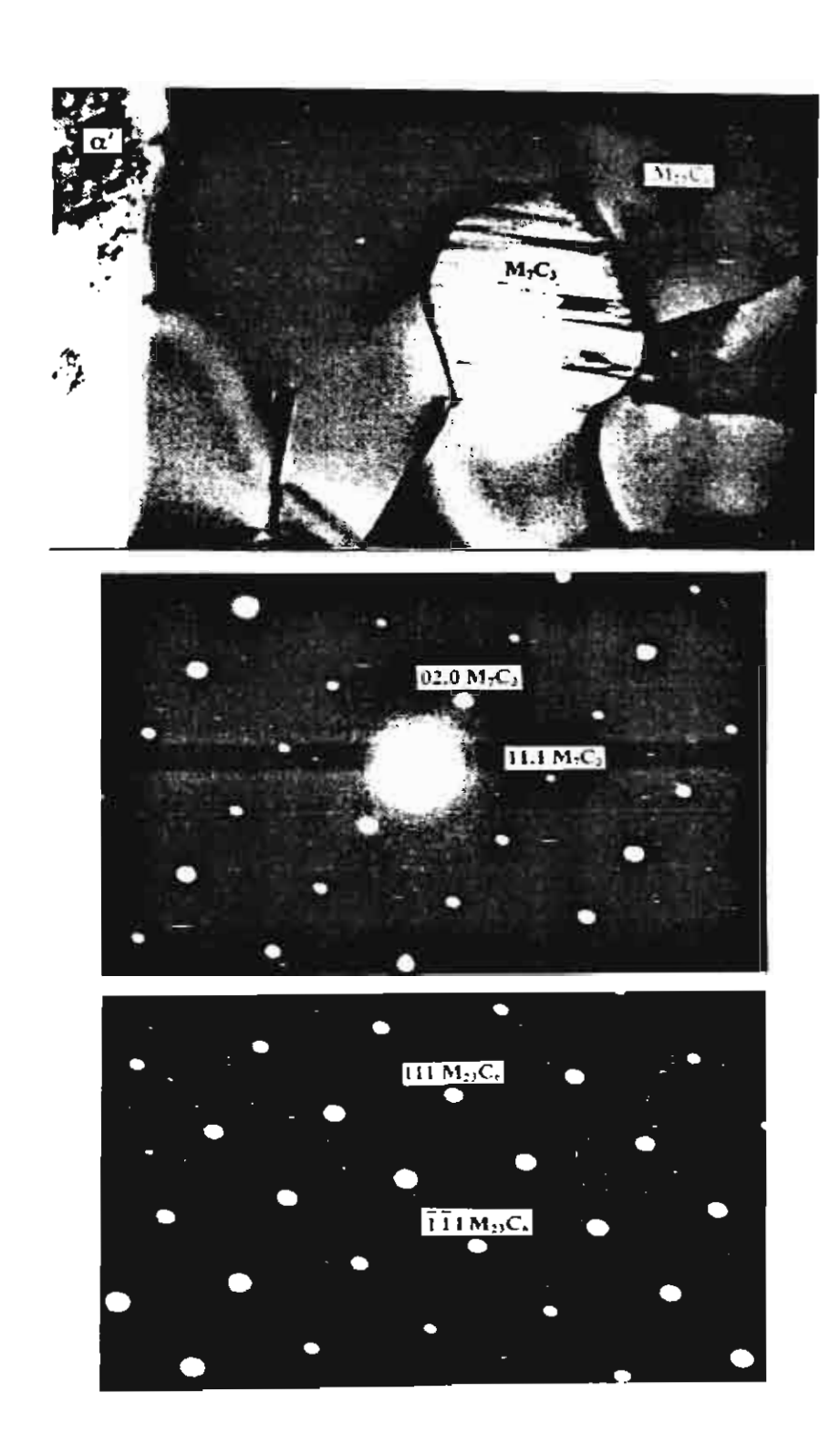
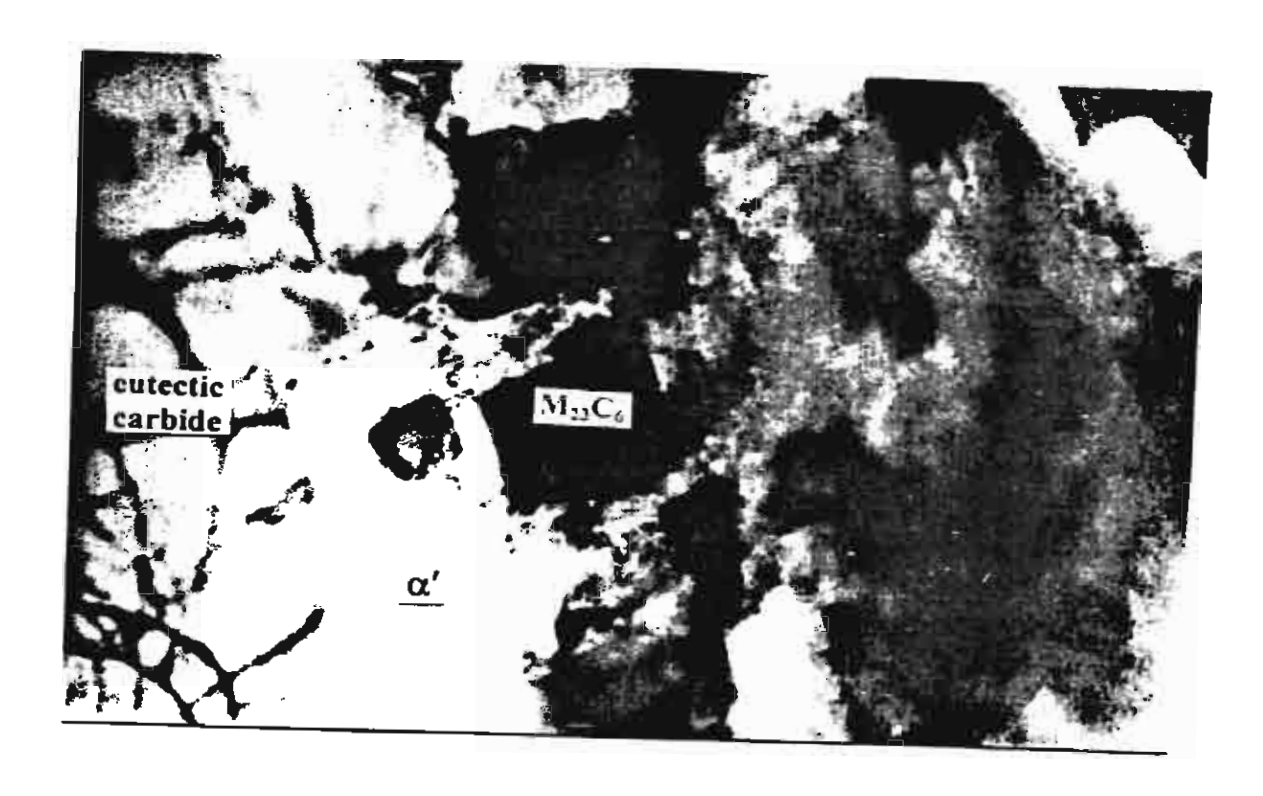


Fig. 8. (a) A bright field TEM micrograph shows a duplex core-shell structure of eutectic carbides. The core area with a faulting contrast is  $M_7C_3$  surrounding by grains of  $M_{23}C_6$ .  $\alpha'$  denotes the martensite matrix. (b) and (c) are corresponding selected area diffraction patterns from  $M_7C_3$  and  $M_{23}C_6$ , respectively. (1025 °C, 4 hours)



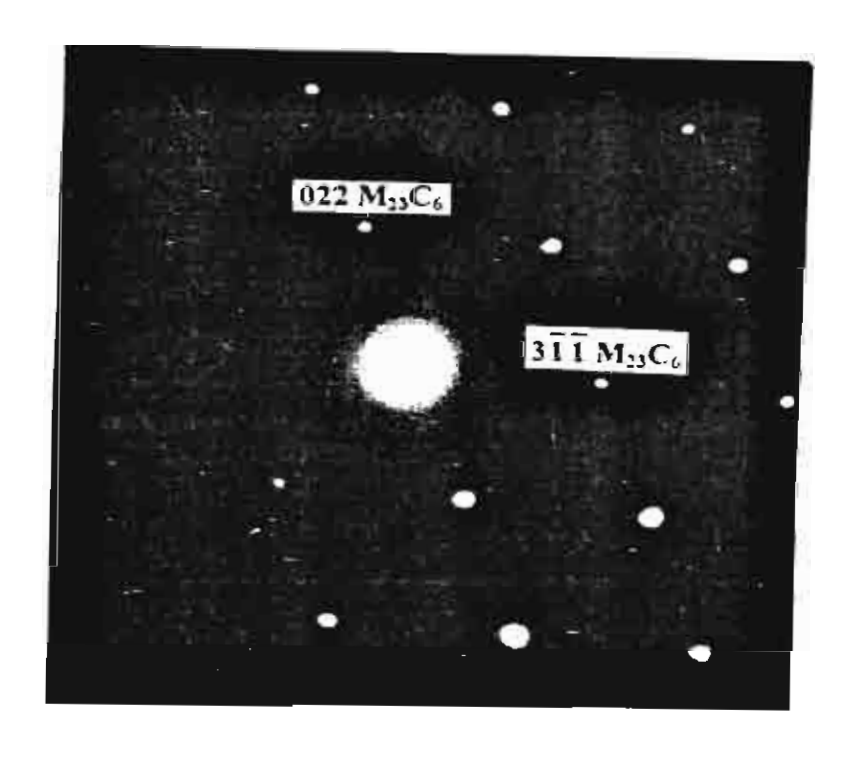


Fig. 9. (a) A bright field TEM micrograph shows secondary carbide particles within the martensite matrix after destabilisation.  $\alpha'$  denotes the martensite matrix. (b) A corresponding selected area diffraction pattern from a particle of secondary  $M_{23}C_6$  carbide. (900 °C, 6 hours)

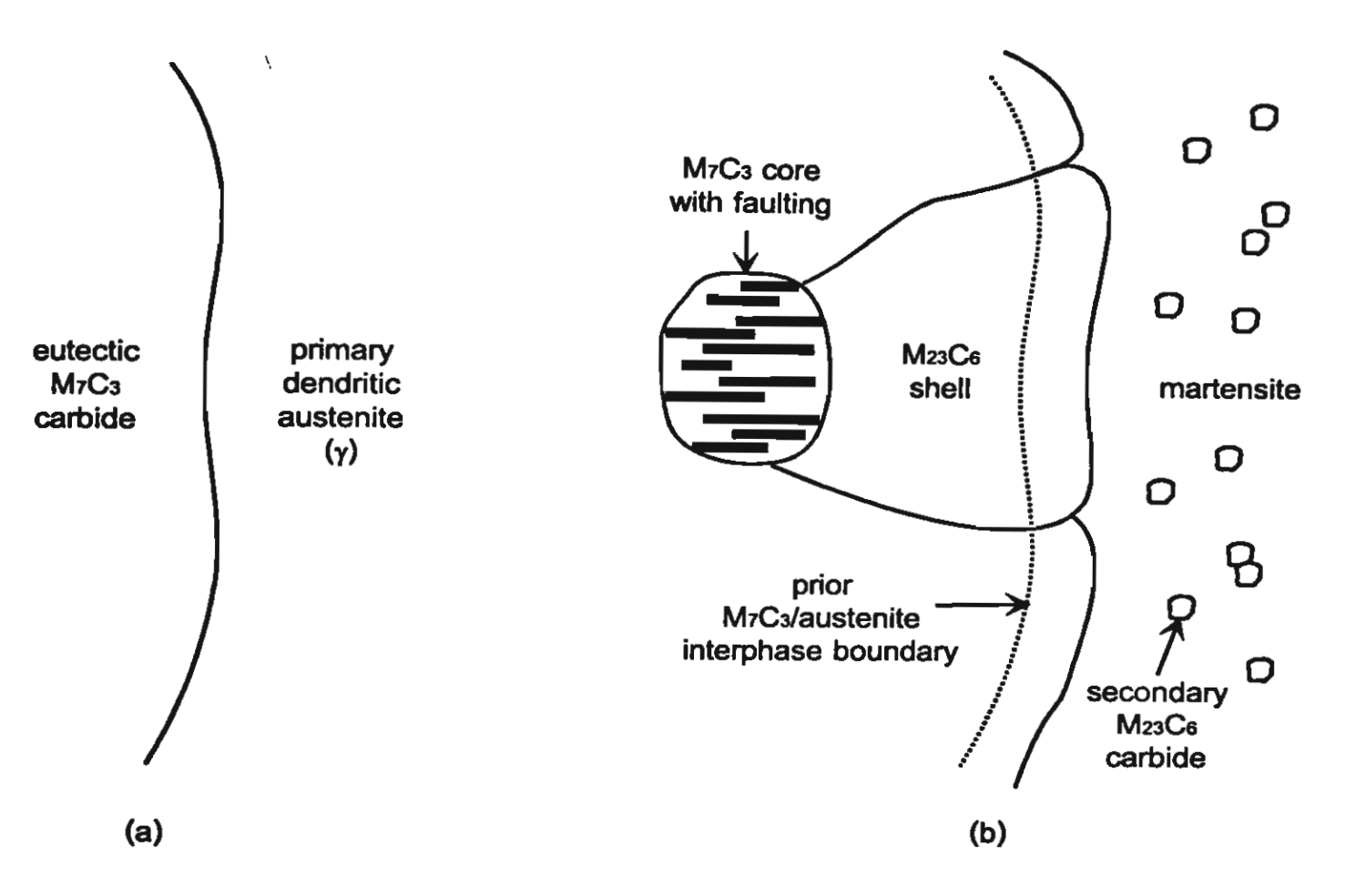


Fig. 10. A schematic illustration suggesting a possible mechanism of  $M_{23}C_6$  shell formation on eutectic  $M_7C_3$  (a) before and (b) after destabilisation heat treatment.

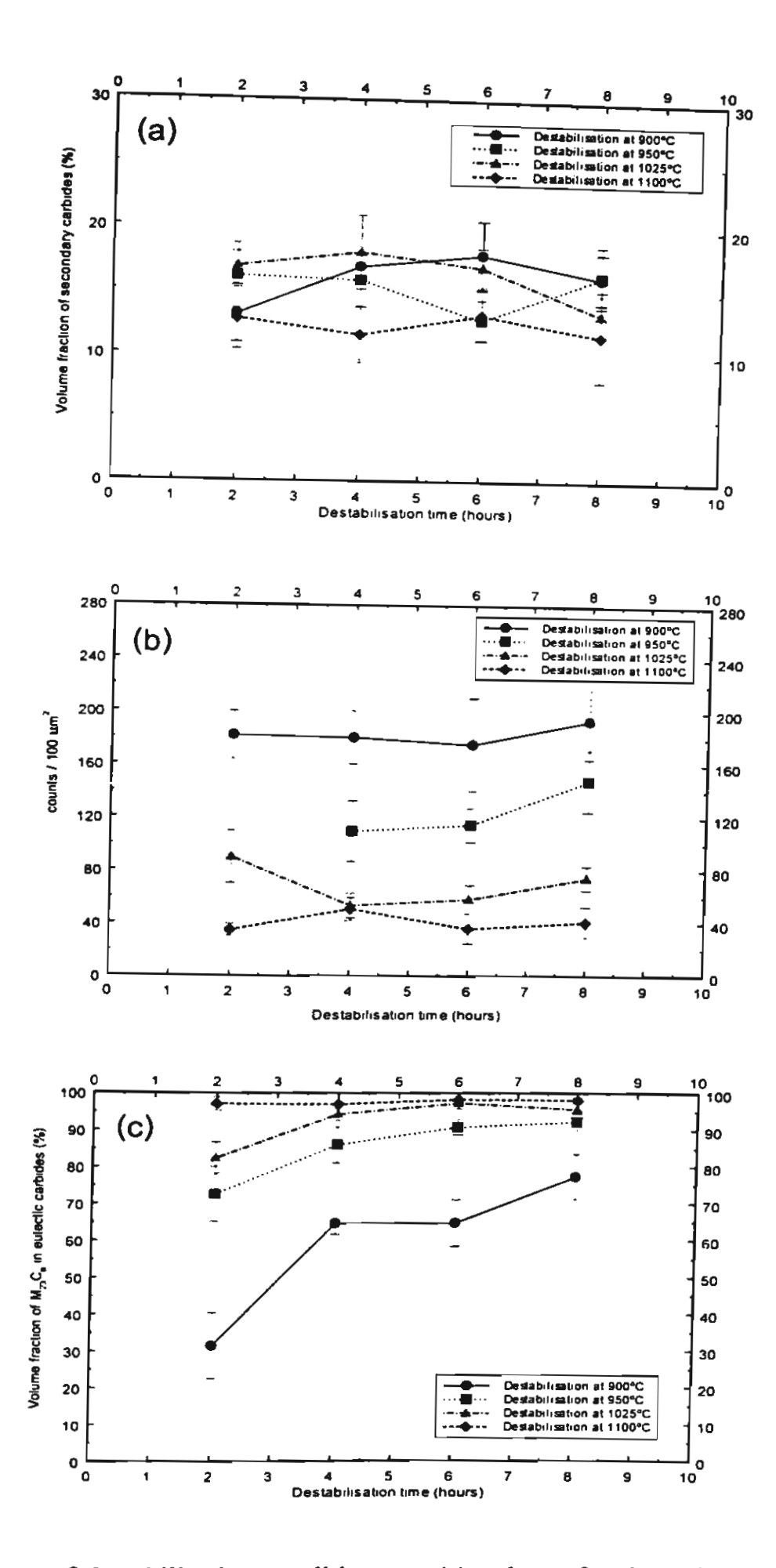


Fig. 11. Effects of destabilisation conditions on (a) volume fraction of secondary carbide, (b) counts per  $100 \, \mu \text{m}^2$  of secondary carbide and (c) volume fraction of  $M_{23}C_6$  in eutectic carbides.

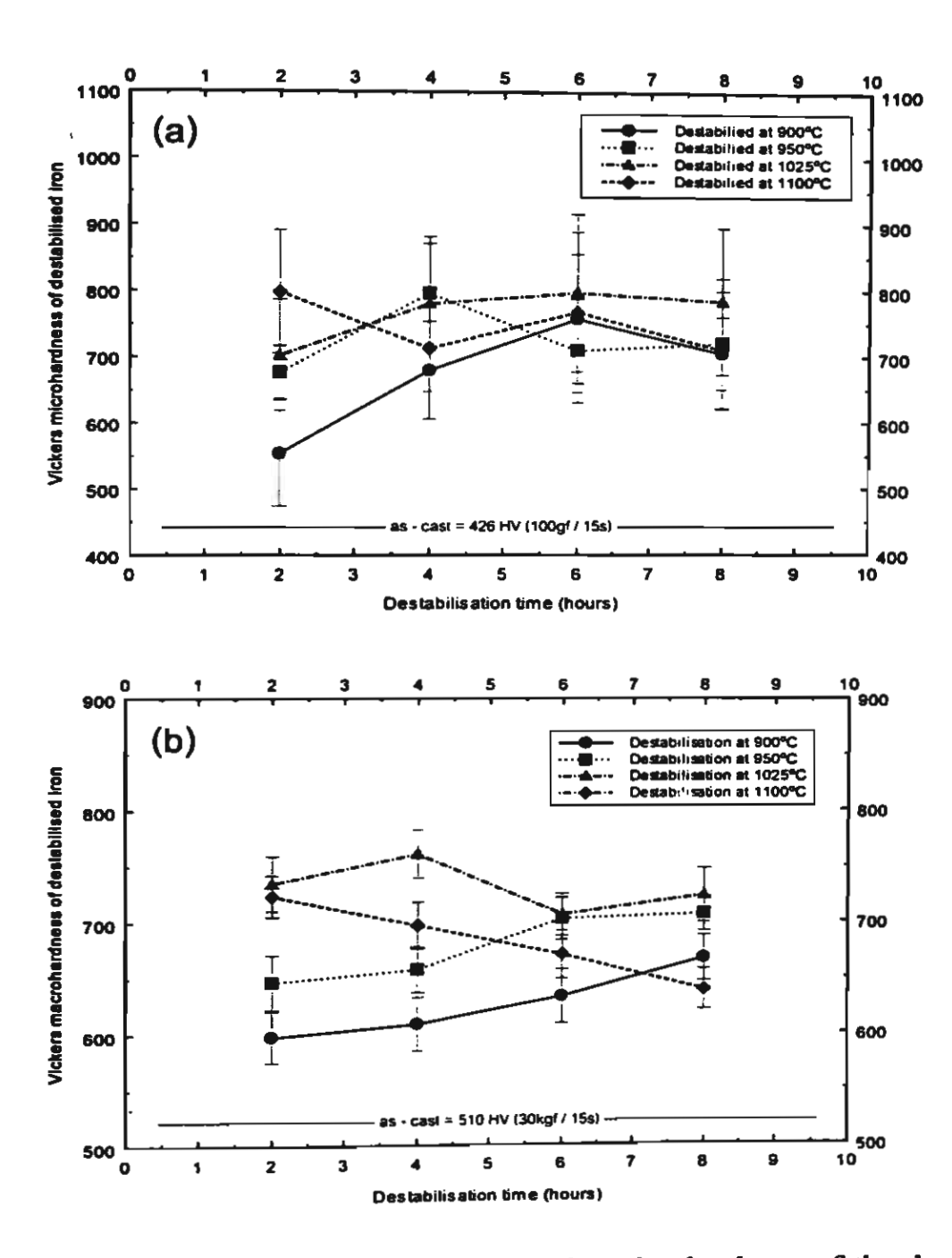


Fig. 12. Effects of destabilisation conditions on (a) the microhardness of the dendritic regions and (b) the overall macrohardness of destabilised iron.

### Characterisation of High Chromium Cast Irons.

Torranin Chairuangsri<sup>1</sup>, Amphorn Wiengmoon<sup>1</sup>, & J.T.H. Pearce<sup>2</sup>.

<sup>1</sup>Department of Industrial Chemistry, Chiang Mai University, Chiang Mai 50200, THAILAND.

<sup>2</sup>MTEC- National Metals & Materials Technology Centre, 114 Paholyothin Rd, Klong 1, Klong Luang, Patumthani 12120, THAILAND. Tel: 66-2-564-6500, Fax: 66-2-564-6403. jthp@mtec.or.th

### ABSTRACT.

High Chromium Cast Irons are one of the main groups of alloys employed to produce cast wear parts. They are extensively used in many industries including mining, coal and mineral processing, cement production, dredging and slurry transport. They are used for many kinds of cast parts ranging from small 10mm diameter grinding cylpebs to much larger castings such as pump bodies, and roller and table segments for roller crushers. For many applications these irons need to be given hardening and tempering heat treatments to develop their optimum resistance to wear and impact loads in service, they may also need to be annealed to allow tool machining prior to hardening.

The physical metallurgy underlying the development of cast microstructures in these irons, and their structural modification by thermal treatments is relatively complex. Structural characterisation via electron microscopy therefore has a key role to play in furthering our understanding of the phase transformations that control their microstructures and hence their service performance as wear parts.

This paper shows how both Scanning and Transmission Electron Microscopy and their associated micro-analytical techniques can provide valuable information not only on the nature of eutectic and secondary carbides and matrix structures in these irons but also on their behaviour during wear and corrosion. Particular attention is given to current research on the  $M_7C_3$  to  $M_{23}C_6$  transformation in eutectic carbides during the heat treatment of 30%Cr irons that have been developed for applications involving corrosive wear e.g. slurry pumps.

### INTRODUCTION.

The wear and fracture behaviour of High Cr Cast Irons depends on the type, proportion and morphology of hard eutectic and precipitated carbides within their microstructures and on the nature of the supporting matrix (1,2). The carbide types known to be present in the Fe-Cr-C system are M3C, M7C3 and M23C6 (3,4). Additional carbide forming elements such as molybdenum, manganese and vanadium are soluble in both M3C and in M7C3, and they may also give rise to other types including M2C and M6C. Elements such as nickel and copper have little solubility in the carbides and remain in solution in

the matrix. Together with Mo, Cu and Ni are used to increase hardenability during heat treatment or to assist in the formation of as-cast austenitic matrix structures (5,6).

Most commercial wear resisting irons are hypo-eutectic and hence solidify as primary austenite dendrites followed by a eutectic of austenite + M7C3. In irons containing less than 12% Cr M3C carbide with a hardness of around 1000Hv is present, below about 6% Cr this carbide is in a continuous form and the irons have reduced toughness. At 8-10% Cr the eutectic carbides become duplex, consisting of M7C3 and M3C, and less continuous, (7). Above 12% Cr the eutectic carbide is completely M7C3, this is fibrous with reduced continuity and has a higher hardness of around 1400-1600 Hv providing improved fracture toughness and wear performance when compared to the lower Cr irons. The eutectic carbide morphology in a 5% Cr and in a 30% Cr iron can be compared in Figure 1.

In high Cr irons the austenite formed on solidification may be retained on cooling in the mould or it may partially or fully transform to ferrite and carbides (secondary and/or pearlitic) or partially transform to martensite depending on composition and cooling rate. Austenitic structures are promoted by faster cooling rates, by high Cr/C ratios, and by Ni, Cu and Mo additions. Due to local C and Cr depletion adjacent to the eutectic carbide there is always some transformation of the eutectic austenite to martensite in as-cast austenitic irons, as illustrated in Figure 2(a).

In some applications as-cast austenitic irons can be used without any hardening heat treatment since the austenite can work harden to provide self-replacing wear resistant surfaces in a similar manner to high Mn steels. However in most cases the irons need to be heat treated (8,9):

- To soften the casting for machining e.g. for roller tyres and pump parts. This
  produces pearlitic and secondary carbides in a ferrite matrix, lowering hardness levels
  down to 350-400Hv.
- To harden via destabilisation treatment (at 950-1050C), air quenching and tempering (at 450-550C). This gives a distribution of secondary carbides in a tempered martensite matrix with small amounts (ideally <5%) of residual austenite: hardness levels are 700-850Hv. Secondary carbides are seen in Figure 2(b).
- To improve toughness by high temperature treatment at 1130-1180C. This produces a controlled amount of secondary carbide precipitation in a fully austenitic matrix and provides fracture toughness levels of 40-45 MPa√m as against 20-30 MPa√m for ascast or normally hardened irons (10,11)

To further develop alloy compositions and heat treatments for cast wear parts the fine scale microstructural features introduced above must be accurately characterised. Although wear damage (12-14) and fracture behaviour (15-17) have been studied extensively by scanning electron microscopy (SEM) there has been less attention given to microstructural characterisation by SEM and by transmission electron microscopy (TEM) and their related micro-analytical techniques. TEM investigation has been restricted by the difficulties in producing satisfactory thin foil specimens in which there is uniform thinning of both carbide and matrix constituents (18-21). Specimen preparation and some

of the theoretical aspects of the use of electron optical techniques to study carbides are covered in a previous paper (22), the present work concentrates on the application of EM techniques in furthering our understanding of microstructure-behaviour relationships in high Cr irons. Some novel work on the application of Electron Energy Loss Spectroscopy (EELS) in the identification and analysis of carbides is also introduced.

To foundries EM techniques may seem far removed from castings production but they do provide the only means by which the high resolution imaging, structural analysis (via electron diffraction) and chemical analysis (via X ray spectroscopy) that are needed for complete structural characterisation of these complex irons can be obtained.

### REFERENCES.

- 1. J.T.H. Pearce, AFS Transactions, Vol. 92, 1984, pp. 599-622.
- 2. J.T.H. Pearce, The Foundryman, Vol. 95, 2002, pp. 156-166.
- 3. R.S. Jackson, Journal of the Iron and Steel Institute, Vol.208, 1970, pp. 163-167.
- 4. AUS Thorpe
- 5. F. Maratray, AFS Transactions, Vol. 79, 1971, pp. 121-124.
- J. Dodd & J.L. Parks, AFS International Cast Metals Journal, Vol.5, 1980, pp. (3) 47-54 and (4) 15-25.
- 7. W.R. Thorpe & B. Chicco, Materials Science & Engineering, Vol. 51, 1981, pp. 11-19.
- 8. J.T.H. Pearce & D.W.J. Elwell, Proceedings of "Best Practices in the Production, Processing and Thermal Treatment of Castings", Cast Metals Developments, 1995, Singapore, pp. 26/1-18.
- 9. J.T.H. Pearce, Metal Casting Technologies, Vol.47, 2001, pp.41-43.
- 10. R.W. Durman, International Journal of Mineral Processing, Vol.22, 1988, pp. 381-399.
- 11. A. Kootsookos, J.D. Gates & R.A. Eaton, Cast Metals, Vol.7, 1994, pp. 239-246.
- 12. J.T.H. Pearce, British Foundryman, Vol.78, 1985, pp. 13-23.
- I.R. Sare, B.K. Arnold, G.A. Dunlop, & P.G. Lloyd, Wear, Vol. 162-164, 1993, pp. 790-801.
- 14. G.J. Gore & J.D. Gates, Wear, Vol. 203-204, 1997, pp. 544-563.
- 15. K.H. Zum Gahr & W.G. Scholz, Journal of Metals, Vol. 32, 1980, pp. 38-44.
- 16. R.W. Durman, British Foundryman, Vol.74, 1981, pp. 45-55.
- 17. S.B. Biner, Canadian Metallurgical Quarterly, Vol. 24, 1985, pp. 155-167.
- 18. V. Biss, Microstructural Science, Vol. 7, 1979, pp.411-421
- 19. J.T.H. Pearce, Journal of Materials Science Letters, Vol.2, 1983, pp. 428-432.
- 20. J.T.H. Pearce, Wear, Vol.89, 1983, pp. 333-344.
- 21. S.K. Hann, J.D. Gates & J.V. Bee, Journal of Materials Science, Vol.32, 1997, pp. 3443-3450.
- 22. T. Chairuangsri & J.T.H. Pearce, Journal of the Electron Microscopy Society of Thailand, Vol.14, 2000, pp. 29-46.